Simulation and characterization of the effect of an eccentric pipe in a cross flow turbine

Endashaw Tesfaye Woldemariam

A Thesis submitted to

The Department of Mechanical Engineering

Mechanical Design Stream

Presented in Partial Fulfillment of the Requirements for the Degree of Masters of Science

Addis Ababa University

Institute of Technology

Addis Ababa, Ethiopia

January, 2013

Addis Ababa University

School of Graduate Studies

This is to certify that the thesis prepared by Endashaw Tesfaye, entitled: Simulation and characterization of the effect of an eccentric pipe in a cross flow turbine and submitted in partial fulfillment of the requirements for the degree of Master of Science complies with regulations of the University and meets the accepted standards with respect to originality and quality.

Signed by the Examining Committee:

Examiner _____Signature _____ Date _____

Examiner _____Signature _____ Date _____

Adviser _____Signature _____ Date _____

_____

Chair of Department of Graduate Program Coordinator

Abstract

In this research a typical practical T15-300a type cross flow turbine is used as a model and four different eccentric pipe diameters are used to numerically simulate and characterize their effect on the fluid flow inside the turbine at three different guide valve angle position. Also a specific flow parameter is taken from a practical site survey at Janbaria river, a tributary of Kesem river, in Amhara Region; for all models. Totally twelve model cases are used for simulation purpose.
The T15-300a model is drawn using a SOLIDWORKS 2012 student version package to give the physical model.

A student version software package of GAMBIT and FLUENT software is used to analyze the numerical simulation for all the models developed initially in SOLIDWORKS software.

Using the numerical simulation results obtained on contours of static pressure, contours of dynamic pressure, contours of velocity magnitude, contours of radial velocity and velocity vectors colored by static pressure and velocity magnitude inside the fluid interior for all models are compared and analyzed.
In this specific paper a Cartesian coordinate system is used for numerical modeling of the cases and simulates and analyzes the result.

As the simulation result show, when increasing the eccentric pipe diameter at any guide valve position has an effect of decreasing most of the flow parameters such as static pressure, dynamic pressure, velocity magnitude and radial velocity.
Also as obtained from velocity vectors diagram increasing the eccentric pipe diameter has an effect of diverting the fluid entering to the second stage of crossed flow. Totally increasing an eccentric pipe diameter decreases the hydraulic energy inside the fluid interior for the given flow parameter, which implies that the hydraulic energy changed to some other energy form, in our case to mechanical power as obtained result from print result values of force moments.

Acknowledgment

My best heart felt gratitude goes to my advisor Dr. Daniel Tilahun for his support and follow up throughout the thesis work regardless of other department loads he carry on while advising me, also for his patience at my on-off times due to inconveniences happened by personal cases.

My heart felt gratitude also goes to Ato Nebiyou Assefa, president of Ethiopian hydropower society for providing me the manufacturing drawing document of T15-300a cross flow turbine. Without his positive attitude to give me the document I wouldn't go a step on this specific thesis.

I also need to acknowledge Dr. Ing. Zewdu and Dr.Ing.Tamirat, internal and external examiners, for their intensive comment on my final thesis document and their suggestion at the time of presentation.

I would also like to extend my best regards to my brothers specially Kumye for being at my side in the time of madness and providing the most necessary equipment for the thesis and the whole postgraduate course work.

My families and friends are also the ones who should be regarded for their day to day belongingness in good and bad moments of mine.

Table of Contents

List of figures

List of tables

Nomenclatures

C - Nozzle (guide valve) profile coefficient

V – Actual water velocity

HP - horse power

ω - Angular velocity of rotor (rad/s)

u - Peripheral velocity

α - the angle that actual velocity of water makes with a line tangent to periphery of the rotor

β - The angle that the relative velocity makes with the peripheral velocity

ψ - Empirical coefficient that relate the relative velocities at the outlet of the first state to the inlet of the second stage

υ - Relative velocity of the fluid inside the turbine

Q - Flow rate of fluid

e - Horse power efficiency

H- Head of fluid

p_d = dynamic pressure (Pa)

ρ = density of fluid (kg/m^3)

v = velocity (m/s)

CFD- computational fluid dynamics

D45v0 – model of eccentric pipe diameter of 45mm at guide valve angle of 0°

D60v0 – model of eccentric pipe diameter of 60mm at guide valve angle of 0°

D100v0 – model of eccentric pipe diameter of 100mm at guide valve angle of 0°

D135v0 – model of eccentric pipe diameter of 135mm at guide valve angle of 0°

D45v16 – model of eccentric pipe diameter of 45mm at guide valve angle of 16°

D60v16 – model of eccentric pipe diameter of 60mm at guide valve angle of 16°

D100v16 – model of eccentric pipe diameter of 100mm at guide valve angle of 16°

D135v16 – model of eccentric pipe diameter of 135mm at guide valve angle of 16°

D45v23 – model of eccentric pipe diameter of 45mm at guide valve angle of 23°

D60v23 – model of eccentric pipe diameter of 60mm at guide valve angle of 23°

D100v23 – model of eccentric pipe diameter of 100mm at guide valve angle of 23°

D135v23 – model of eccentric pipe diameter of 135mm at guide valve angle of 23°

$\vec{a}$ = specified force vector

$\vec{F}_p$ = pressure force vector

$\vec{F}_v$ = viscous force vector

A = specified moment center

B = force origin

$\vec{r}_{AB}$ = moment vector

Chapter one: Introduction

1.1 Back ground of the study

Rising oil prices, increasing global energy consumption and concern for the environment has led to a renewed interest in alternative energy sources such as renewable energy. Renewable energy currently constitutes about 17% of the global energy mix with hydropower making about 90% of this and it makes about 20% contribution to the global electricity supply, second to fossil fuel. It is anticipated that the global demand for electricity will increase steadily and the growth for hydroelectricity is projected at 2.4%–3.6% from 1990–2020. The technically feasible hydropower potential of Africa is around 1,750TWh which is about 12% of the global capacity. Only 5% of this technically feasible potential is exploited. Hydropower potential of the continent is estimated around 100, 000 MW of this small hydro power potential constitute large of this amount. [1] Considering the substantial hydropower resources, Ethiopia has one of the lowest levels of per capita electrical consumption in the world. Out of hydropower potential of about 15,000-30,000 MW, only about 360 MW (i.e. less than 2 percent) has been exploited by 1997.[2].

Small-scale hydropower was the most common way of electricity generating in the early 20th century. The first commercial use of hydroelectric power to produce electricity was a waterwheel on the Fox River in Wisconsin in 1882 that supplied power for lighting to two paper mills and a house. Though different countries have different criteria to classify hydro power plants scale, the most general classification of hydro power plants shows that small hydro plants have power ranges below 1 MW in which 5Kw-100KW is categorized under micro hydro powers. [3]

Of all the non-conventional energy resources small hydro represents the highest density of resource. Global installed capacity of Small hydro is around 50, 000 MW against the estimated potential of 180 000MW (Baidya, 2006). Due to its short gestation period, small hydro is attracting worldwide attention. [1] Several solutions have been proposed and successfully implemented for micro-hydro schemes, which include radial flow turbines and axial flow propeller type turbines. At present, the cross-flow hydraulic turbine is gaining popularity in small and ultra-low head establishments due to its remarkably simple structure and the ease of manufacturing that it provides. The cross-flow turbine was invented about a century ago. The

cross-flow hydraulic turbine is composed of two major parts, the runner and the nozzle. The water jet leaving the nozzle strikes the blades at the first stage. The water exits the first stage and is 'crossed' to the second stage inlet after which it exits the runner completely. Some of the water is entrained between the turbine stages and does not contribute to the energy generation. [4]

1.2: Statement and purpose of the problem

Though there are an incredibly high potential of micro hydro power resources, and known that cross flow turbine is widely used to exploit the available fluid power because it is simple to manufacture using locally available technologies with lower capital, its efficiency (performance) is very low when compared to other turbine types as of today's current situation. Besides out of the total power tapped by it, which is around 68-70%, only around 32% is obtained from the second stage fluid power.

The purpose of this study is to simulate the cross flow turbine model using CFD modeling and obtain characteristic effect of an eccentric pipe that is used to guide the fluid coming out from the 1st stage which aimed to improve the exploitation of a better performance from the second.

1.3: Objectives of the research

Thus, the major objective of this thesis is to

- Simulate and characterize the effect of different size eccentric pipe located eccentrically at the middle of the rotor so that it directs the water jet leaving the inner periphery from the 1st stage to give a better striking angle at the entry of the second stage.

The minor objectives of the project are to

- characterize and analyze the velocity contour with different physical and flow parameters
- characterize and analyze the static and dynamic pressure contour with different physical and flow parameters
- characterize and analyze the velocity vector colored by velocity magnitude and static pressure

1.4: Research methodology

The following methodologies will be used to fulfill the above objectives

A) An intensive survey of literature about cross flow turbine rotor efficiency, nozzle profile, and blade curvature

B) Numerical modeling of the cross flow turbine in SOLIDWORKS, setting the boundary conditions and meshing using GAMBIT and solving using a better and locally available version of FLUENT software. Then

- Characterization of the effect of different eccentric pipe diameter for the given

  - Blade curvature
  - Nozzle profile and angle

- Characterization of crossed fluid for the

  - Eccentric pipe diameter
  - Blade curvature
  - Nozzle profile and angle

- Characterization of performance of the turbine rotor for the

  - Eccentric pipe diameter
  - Blade curvature
  - Nozzle profile and angle

C) Analysis, interpretation and characterization of the result for the fluid flow parameter under consideration

1.5: Expected research outcomes

For fluid power and turbine models under consideration

- An efficient eccentric pipe diameter range will be obtained
- A better guide valve position range will be indicated
- The second stage fluid power will be increased
- And optimized and efficient crossed flow micro hydro turbine will be proposed with the better eccentric pipe diameter range.

Chapter two: Literature review

Several researchers undergone researches to optimize and increase the performance of a cross flow turbine using different methods, analyzing that improving efficiency saves a lot of hydrolic power loss at hydropower sites and most of them focusing on the nozzle and runner part of the turbine. Also computational fluid dynamic (CFD) modeling is used to characterize different basic parameters of the turbine. Some of the researches undergone and found at hand are described below:

Proff. C.A. Mockmore and proff. Fred Meryfield Stated in their Banki Turbine paper undergoing a laboratory experiment with a rectangular nozzle with the inlet water striking the turbine blade at an angle of 16°, obtained 68% efficiency and also known that 8% of the total water never touched the wheel. Also found that the effective width of the wheel can be changed at will with out changing the angle of attack. They felt that more efficiency could be obtained by experimenting with different number of blades and different nozzles. [5]

Jusuf Haurissa, Rudy Soenoko on their experimental research on performance and flow characteristics lattitude of nozzle in turbine blades second level; Initial experiments, were carried out to design a nozzle blade on the blade enter the second level. In their study concluded in the best of flow turbine blades latitude, using nozzle on the second level entry was better than without using the blade entry nozzle on the second level. In the best flow turbine blade latitude, using nozzle on the second level, the result was in efficiency 74,68 %, which was larger than the first, second, and three test (the first test used the first and second generation efficiency 63,46% , second best uses only. The first generation efficienct 52,49 %, a third test used only the generation of second level efficiency 44,92 %. The difference efficiency that was resulted was the second one, which was 11,2 %, 22,2 %, 29,76 %. The design of a new cross flow turbine with nozzle angle on the blades enter the first level of 32° and angel of entry nozzle at the blade entry second level of 200. The design of nazzle on the blades into the second level, could be used for model cross flow turbine (cross flow turbine) of any kind. [6]

Numerical analysis of the internal flow in a hydraulic cross-flow turbine type Banki was also studied by Jes´us De Andrade, Christian Curiel, Frank Kenyery and Orlando Aguill . A 3D-CFD

steady state flow simulation has been performed using ANSYS CFX codes. The simulation includes nozzle, runner, shaft, and casing. Simulations were carried out using a water air free surface model and k-ε turbulence model with an objective to analyze the velocity and pressure fields of the cross-flow within the runner and to characterize its performance for different runner speeds. They have found that using CFD techniques, it was possible to simulate the behavior of the 3D steady state free surface flow (water-air) inside the nozzle-casing assembly of the turbine, being able to visualize the flow field and to obtain the flow angles along the nozzle outlet. It was also found that the flow angles along the nozzle outlet $\alpha 1$ that would come into the 1st stage of the runner slightly varies from 23◦ to 7◦ along the rotation angle θ, passing through the design condition angle $\alpha 1$ = 16◦. The water volume fraction was also addressed. The results show that the admission arc is full of water from 5° of the rotation angle. The percentages of energy transfer in the 1st and 2nd stage were addressed for the design speed. The results show that 68.5% percent of the energy transferred occurs in the 1st stage, and the remaining 31.5% is transferred in the 2nd stage. [7]

An experimental investigation was conducted by HAYATI OLGUN to study the effects of some geometric parameters of runners and nozzles (e.g. diameter ratio and throat width ratio) on the efficiency in the cross-flow turbines, by varying of ratio of inner-to-outer diameters of runners and gate openings of two different turbine nozzles under different heads. The blade inlet and outlet angles were selected as 30° and 90°. Nozzles outlet angles of two solid walls of 16° were measured from the circumferential direction. The performance parameters namely output power, efficiency, runaway speed, reduced speed and power for different nozzle/runner combinations were investigated by changing head range from 8 to 30 m, the nozzle A-runner combinations and from 4 to 17 m, the nozzle B-runner combination at different gate openings and the following concluding remarks are extracted: (i) Cross-flow turbines can be operated efficiently in a wider range of gate openings than most turbines. (ii) Maximum efficiency practically occurs at a constant speed for all gate openings at constant head. (iii) The speeds for maximum efficiency changes with increasing the head at constant gate openings. (iv) There is a distinct place for the cross-flow turbine in the micro turbine field. (v) The runner with diameter ratio 0.67 is more efficient than the runners with diameter ratios of 0.54, 0.58 and 0.75. [8]

HAYATI OLGUN also under gone an experiment on the effect of interior guide tube used inside the runner of a cross-flow turbine to collect and guide the crossing flow towards the

second stage of the runner. The interior guide tubes were designed on the basis of observed flow patterns inside the runner. Experimentally, three different types of tubes were tested. The laboratory tests were conducted to calculate the turbine efficiency with different gate openings of nozzle and different positions of interior guide tubes. When the experiments were done with and without interior guide tubes, it has been found that turbine efficiency with the interior guide tube decreased about 5 per cent. [9]

Visiting Asst. Prof., Dept. of Civ. Engrg., Clemson Univ., Clemson, SC 29634-0911 and 2Assoc. Prof., Dept. of Civ. Engrg., Clemson Univ., Clemson, SC undergone a study that discusses an experimental investigation of the key parameters influencing cross-flow turbine efficiency. The experiments included measurements of torque, rotational speed, flow rate, and total head in physical models of turbines and nozzles. One physical parameter (flow rate) and six geometric parameters of the turbine were investigated: the angle of water entry to the runner, diameter ratio, number of blades, flow-stream spreading, runner aspect ratio, and blade exit angle. A total of 39 runners and 11 nozzles were tested in 75 different combinations. Analysis performed on the results identified the impact of the different parameters on the turbine efficiency. The results indicate that with careful selection of the cross-flow turbine parameters, efficiencies as high as 88.0% with an uncertainty of ±2.4% can be achieved. This is considered an improvement over the claimed maximum efficiency reported in the literature. [10]

C.A. Consul, R.H.J Willden, E. Ferrer and M.D. McCulloch on their research on the influence of solidity on performance of cross flow turbine presents a numerical investigation of the influence of solidity on the hydrodynamics of a generic tidal cross-flow turbine. A two-dimensional RANS based CFD model has been used to compare the performances of a two-bladed and a four-bladed cross-flow turbine, with solidities of 0.019 & 0.038 respectively, operating at an average blade Reynolds number of 4.42! 105. The numerical investigations showed that increasing the number of blades from two to four resulted in an increase in the maximum power coefficient from 0.43 to 0.53. However, no account has been taken of drag penalties resulting from additional blade support struts. Furthermore, increasing the number of blades resulted in a reduction in the spatio-temporal mean stream wise flow velocity within the turbine of between 14% and 26% depending on the tip speed ratio. Due to the decrease in stream wise velocity the blades of the higher solidity turbine were presented with lower angles of attack, which resulted in the entire power curve being shifted to lower tip speed ratios. At low tip speed ratios, power take-off is limited by

stalling, so that a decrease in the angle of attack, due to higher solidity, results in an increase in lift and hence power generated, whilst at high tip speed ratios, low angles of attack are the limiting factor, so that a decrease in the angle of attack due to higher solidity results in lower lift and thus power. [11]

Some researchers had also undergone a study on CFD modeling based evaluation showing the effectiveness power of simulation and CFD modeling by comparing the result with experimental results. S Lain and C Osorio carried out a study of unsteady flow around a cross flow water turbine using a transient rotor-stator approximation with a moving mesh technique in turbulent flow. Simulation results are in good agreement with experiments. Also, average torque and power coefficients versus tip speed ratio curves have been constructed for referred turbine. Over all their work demonstrated that CFD model can effectively predict hydrodynamic performance of cross flow water turbines. [12]

Chapter three: Physical model and working principle of cross flow turbine

3.1: Cross-flow turbine

This impulse turbine, also known as Banki-Michell is used for a wide range of heads overlapping those of Kaplan, Francis and Pelton. It can operate with heads between 5 and 200 m.

Water enters the turbine, directed by one or more nozzles located upstream of the runner and crosses it two times before leaving the turbine.

The main characteristics of the cross-flow turbine is the water jet of rectangular cross-section which passes twice through the water blades arranged at the periphery of the cylindrical rotor perpendicular to the rotor shaft. The water flows through the blades first through the periphery towards the center then, after crossing the open space inside the runner, from inside outwards. Energy conversion takes place twice; first up on impingement of water on the blades up on entry, and then when water strikes the blades up on exit from the runner.

The Cross-flow turbines have low efficiency compared to other turbines and the important loss of head due to the clearance between the runner and the downstream level should be taken into consideration when dealing with low and medium heads. Moreover, high head cross-flow runners may have some troubles with reliability due to high mechanical stress.

It is an interesting alternative when one has enough water, defined power needs and low investment possibilities, such as for rural electrification programs.

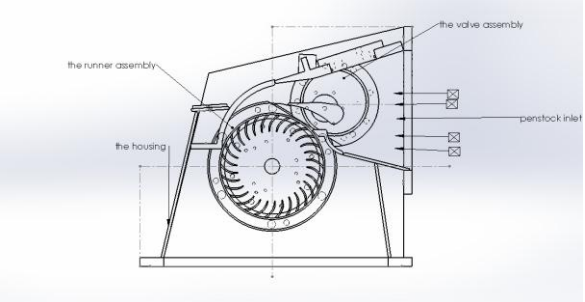

Figure 1: Cross flow turbine system assembly

3.2: The Nozzle (guide valve or distributer)

The water that comes from the source through the penstock is guided by the nozzle before it hits the turbine runner. This nozzle determines the inlet water angle to strike the blade of the rotter. Different designers and researchers use different nozzle profile for different hydropower range and draft tube alignment. And nozzle alignment angle is controlled by a device outside the housing manually.

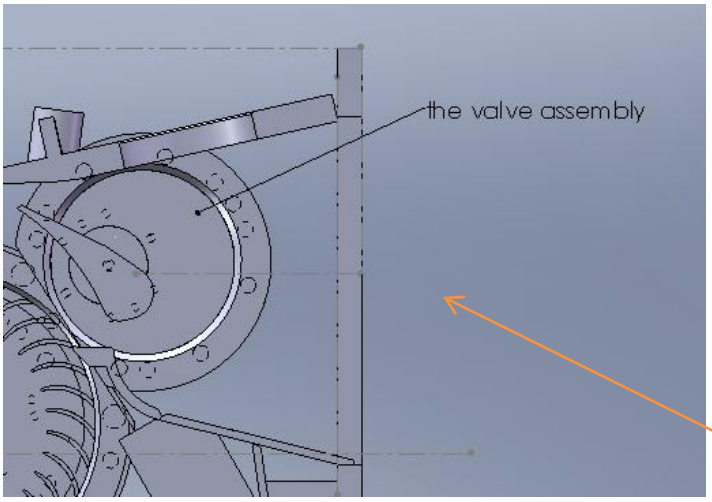

Figure 2: Nozzle and penstock inlet assembly

3.3: Turbine rotor (blade and pipe)

Cross-flow turbine runner is composed of three parts, blade, side and intermediate plates, and the shaft. The water guided by the nozzle will strike the runner blade at an angle designed. The crossed water that comes out from the first stage will again strike the other side blade of the runner.

Several researchers undergone researches to optimize and increase the performance of a cross flow turbine using different methods, analyzing that improving efficiency saves a lot of hydraulic power loss at hydropower sites and most of them focusing on the nozzle and runner part of the turbine. Also computational fluid dynamic (CFD) modeling is used to characterize different basic parameters of the turbine.

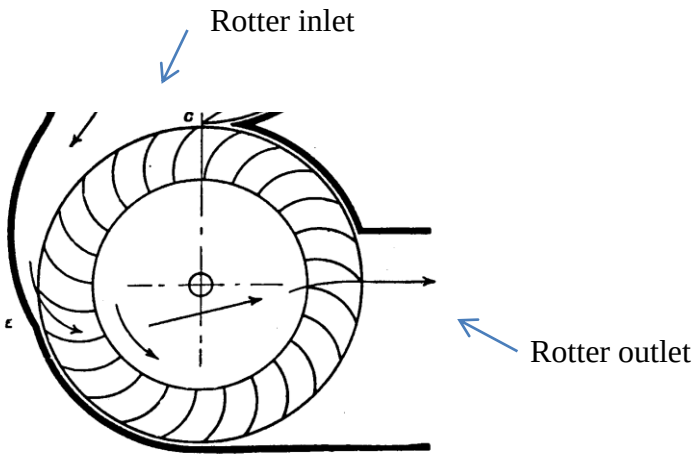

Figure 3: Cross-flow turbine runner part

This study mainly tries to investigate the optimum size of an eccentric pipe at the center of the rotor that provides a considerably better performance to the turbine performance using CFD. To undergo this research the investigations from previously done researches are used.

3.4: T15-300a cross flow turbine commercial design model

A T15-300a cross flow turbine is a commercial design licensed by ENTEC. The present improved turbine generation, the T15 Turbine, is based on a consequent optimizing process conducted over many years. Numerous computer based modifications of the hydraulic profile were empirically tested in the laboratory of the Institute for Hydraulic Machines of Stuttgart University. This turbine can generate up to 25 Kw power and designed to operate with a rotational speed of 750rpm.

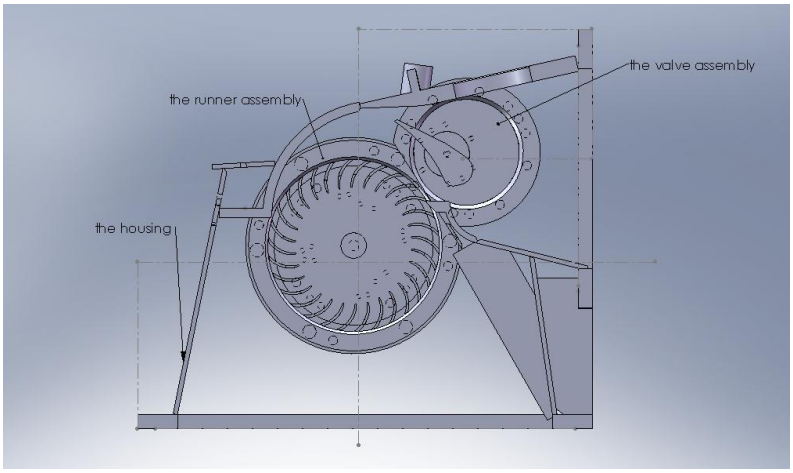

Figure 4:- sectional view of assembled T1-300a model

Basic physical parameter of this specific turbine are indicated below

Rotor outer diameter	300mm
Rotor inner diameter	204.1mm
Inlet nozzle angle	0, 16 as per bank's result, and 23^0
Total Rotor width (all chamber)	408mm (5 disks, 2 side plate disks)
Number of blades	30
Inner blade angle	48^0
Outlet blade angle	90^o from the peripheral tangent line
Nozzle radius of curvature	233.4mm (inner curvature)

From the given parameters of the model and using a particular site survey data, the theoretical power input and expected outputs can be calculated, which apparently provides the efficiency of the model.

3.5: Flow parameters used for analysis of the model

Using a site hydraulic data around Janbaria river, a tributary of Kesem river, in Amhara Region, which currently are using for generation of mechanical power for milling machine.

Flow rate	80(l/s)
Effective head	100m (pressure =981000Pa)

Figure 5: picture of Janbaria river site

The different local models named for the purpose of this thesis are tabulated below

Model	Eccentric pipe diameter (mm)	Guide valve angle (°)
D45v0	45	0
D45v16	45	16
D45v23	45	23
D60v0	60	0
D60v16	60	16
D60v23	60	23
D100v0s	100	0
D100v16	100	16
D100v23	100	23
D135v0	135	0
D135v16	135	16
D135v23	135	23

Table 1: models for case study analysis with different physical parameters (D- represent eccentric pipe diameter and v-represent the guide valve angle)

The following variables were analyzed from model after undergoing the numerical calculation:

1. Grid motion
2. Contours of velocity, a minimum and maximum velocity ranges
    (a) Radial velocity
    (b) Velocity magnitude
3. Contours of pressure, minimum and maximum pressure ranges
    (a) Static pressure
    (b) Dynamic pressure
4. Velocity vectors colored by static pressure
6. XY plot:
    (a) Static pressure vs. position of interior
    (b) Velocity magnitude vs. position of interior
    (c) Static and dynamic pressure vs. curve length of rotor
    (d) Velocity vs. curve length of rotor
6. Print values of moment force on the rotor (blade and eccentric pipe)

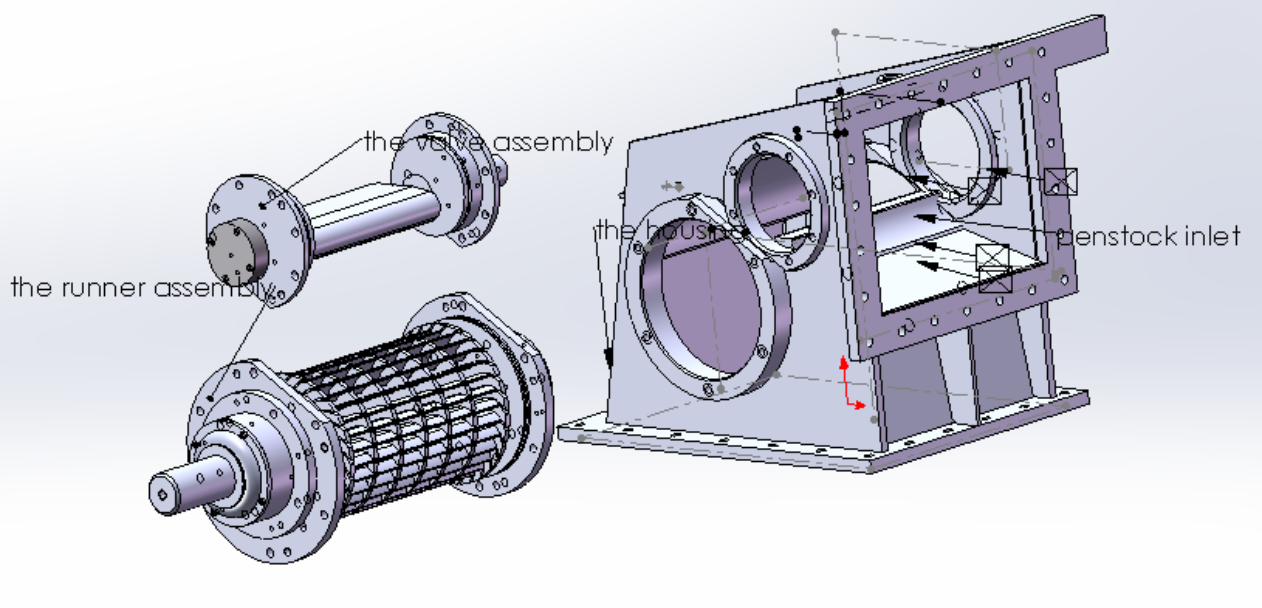

Figure 6:- 3D exploded drawing of the model of the cross flow turbine used for simulation purpose

Chapter four: Mathematical equations for fluid flow in a cross flow turbine

4.1: Theoretical fluid power and efficiency

As it is written under the theory of bank's turbine the path of the jet through turbine assuming that the jet enters the rotor at point A, at an angle of α with the tangent of the periphery, the velocity of the water before entering would be:

$$V_1 = C(2gH)^{1/2} \quad \text{.....(1)}$$

Where, V_1 is the actual inlet velocity

C is the coefficient depend up on the nozzle

H is the actual head of the water

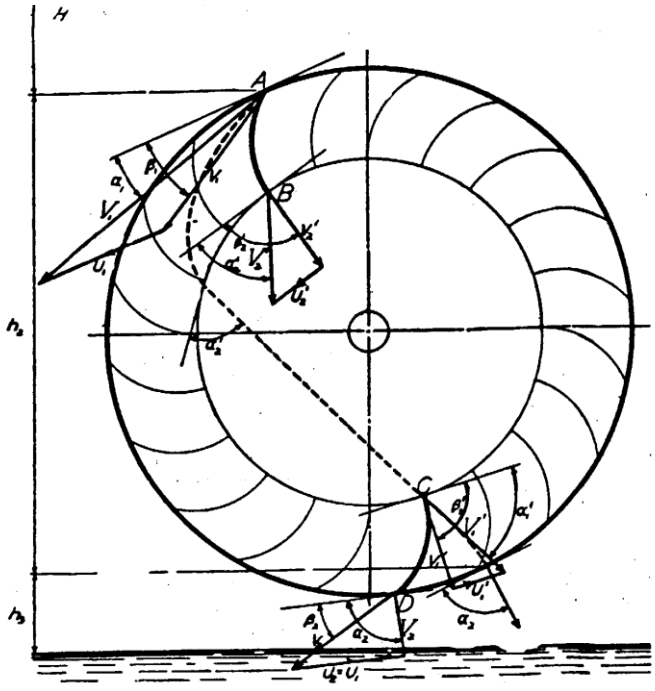

Figure 7:- The water path through the rotor

From conservation of mass & energy and using velocity triangle (shown in the figure 7: below) of turbo machine the theoretical output horse power (HP) calculated from

$$HPo = (\omega Q/g)(V_1 cos\alpha_1 + V_2 cos\alpha_2)u_1, \quad \text{.....(2)}$$

Where: ω is the angular velocity

u_1 is the peripheral velocity at the outer rim and

α_1 & α_2, are the angles of the actual water velocity at the inlet and out let of the rotor

Using the velocity triangles and introducing an empirical coefficient ψ, which in this thesis get more attention due to the eccentric pipe expected to divert the fluid direction leaving the 1st stage, that relates $v_2 = \varphi v_1$, also $\beta_2 = \beta_1$, since they are corresponding angles of the same blades. HPo could be solved as

$$HPo = (\omega Q u_1/g)(V_1 cos\alpha_1 - u_1) \times (1 + \varphi) \quad \text{.....(3)}$$

The theoretical power input due to the head of the water is calculated as

$$HPi = QH\omega/g = \omega Q V_1^2/2gC^2 \quad \text{.....(4)}$$

Therefore, the efficiency of the model can simply be calculated as the of horse power output to the water horse power input.

$$e = {HPo}/{HPi}$$

$$e = (2C^2 u_1/V_1) \times (1 + \varphi)\ (cos\alpha_1 - u_1/V_1) \quad \text{.....(5)}$$

To find the optimum value of efficiency, differentiate e with respect to u_1/V_1 and set equal to zero, considering other terms constant.

It gives, $u_1/V_1 = cos\alpha_1/2$ .....(6)

Then for maximum efficiency

$$e_{max} = \frac{1}{2} C^2 (1 + \varphi) cos^2 \alpha_1 \quad \text{.....(7)}$$

Using equation (6), the given model geometrical parameter and effective water head value

$$u_1 = r\omega \quad => \quad \omega = u_1/r$$

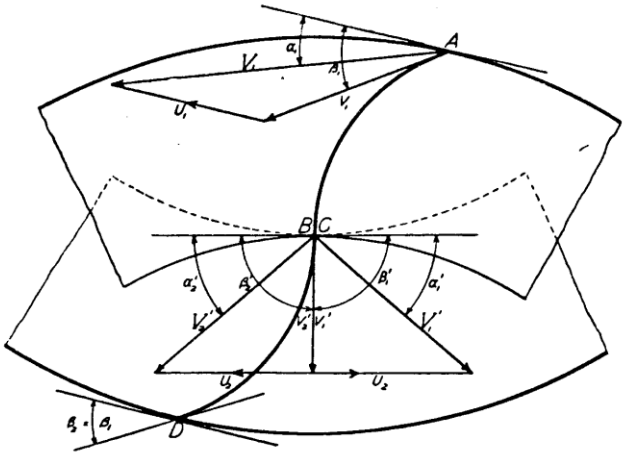

Figure 8: Composite velocity diagram

By using the hydraulic power input calculated using the above equations and estimated efficiency found we can find the theoretical mechanical power transmitted to the turbine, which helps us to calculate the torque on the turbine rotor.

4.2: Terms analyzed from numerical calculation result

4.2.1 Static pressure

The term static pressure is sometimes used in fluid statics to refer to the pressure of a fluid at a nominated depth in the fluid. Thus to find the inlet boundary condition pressure the following pressure formula is used which helps to get pressure from a given head of fluid.

$P=\rho gH$ ……..(8)

Where ρ- is density of fluid considered

H- Head of fluid

4.2.2 Dynamic pressure

Dynamic pressure is a defined property of a moving flow of fluid and can be expressed as

$p_d = 1/2\ \rho\ v^2$ ……(9)

where p_d = dynamic pressure (Pa)

ρ = density of fluid (kg/m^3)

v = velocity (m/s)

4.2.3 Pressure moment

The total force component along the specified force vector $\vec{a}$ on a wall zone is computed by summing the dot product of the pressure and viscous forces on each face with the specified force vector. The terms in this summation represent the pressure and viscous force components in the direction of the vector $\vec{a}$:

$$\underbrace{F_a}_{total\ force\ component} = \underbrace{\vec{a}\cdot\vec{F}_p}_{pressure\ force\ component} + \underbrace{\vec{a}\cdot\vec{F}_v}_{viscous\ force\ component} \quad \text{.....(10)}$$

where

$\vec{a}$ = specified force vector

$\vec{F}_p$ = pressure force vector

$\vec{F}_v$ = viscous force vector

The total moment vector about a specified center A is computed by summing the cross products of the pressure and viscous force vectors for each face with the moment vector $\vec{r}_{AB}$, which is the vector from the specified moment center A to the force origin B. The terms in this summation represent the pressure and viscous moment vectors:

$$\underbrace{\vec{M}_A}_{total\ moment} = \underbrace{\vec{r}_{AB}\times\vec{F}_p}_{pressure\ moment} + \underbrace{\vec{r}_{AB}\times\vec{F}_v}_{viscous\ moment} \quad \text{.....(11)}$$

where

A = specified moment center

B = force origin

$\vec{r}_{AB}$ = moment vector

$\vec{F}_p$ = pressure force vector

$\vec{F}_v$ = viscous force vector

$\vec{F}_v$ = viscous force vector

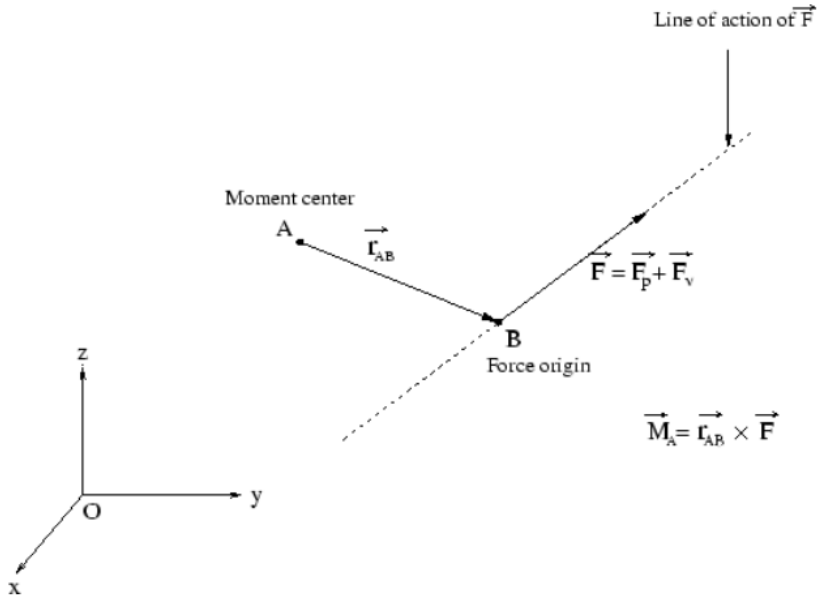

Figure 9: Moment about a Specified Moment Center

Furthermore, the moments along a specified axis are computed. These moments, also known as torques, are defined as the dot product of a unit vector in the direction of the specified axis and the individual and net values of the pressure, viscous, and total moments and coefficients.

Chapter five: Numerical modeling of cross flow turbine

5.1: Computational fluid dynamics

The ultimate goal of the field of computational fluid dynamics (CFD) is to understand the physical events that occur in the flow of fluids around and within designated objects. These events are related to the action and interaction of phenomena such as dissipation, diffusion, convection, shock waves, slip surfaces, boundary layers, and turbulence.

It is generally accepted that the phenomena of importance to the field of continuum fluid dynamics are governed by the conservation of mass, momentum, and energy. The partial differential equations resulting from these conservation laws are referred to as the Navier-Stokes equations. However, in the interest of efficiency, it is always prudent to consider solving simplified forms of the Navier-Stokes equations when the simplifications retain the physics which are essential to the goals of the simulation. Possible simplified governing equations include the potential-flow equations, the Euler equations, and the thin-layer Navier-Stokes equations. These may be steady or unsteady and compressible or incompressible. [13]

Boundary types which may be encountered include solid walls, inflow and outflow boundaries, periodic boundaries, symmetry boundaries, etc. The boundary conditions which must be specified depend upon the governing equations.

Then numerical method and a strategy for dividing the flow domain into cells, or elements, must be selected. Many different gridding strategies exist, including structured, unstructured, hybrid, composite, and overlapping grids. Furthermore, the grid can be altered based on the solution in an approach known as solution-adaptive gridding. The numerical methods generally used in CFD can be classified as finite-difference, finite-volume, finite-element, or spectral methods.

The results of the simulation must be assessed and interpreted. This step can require post-processing of the data, for example calculation of forces and moments, and can be aided by sophisticated flow visualization tools and error estimation techniques.

5.1.1: Governing equations of fluid flow inside the cross flow turbine

The rotation formed by the fluid flow inside the cross flow turbine body can be described by the Navier-Stokes equation; however, the flow is expected to be turbulent. Therefore, the fluid motion and transport characteristics are governed by not only three conservation equations, but also by other additional equations for the turbulent kinetic energy and the rate of dissipation of kinetic energy

FLUENT uses a **Control Volume (CV)** Technique to convert the governing equations into algebraic equations. The control volume technique is the integration of the governing equations in each control volume, yielding discrete equations which conserve each quantity on a control-volume basis

Assumptions used on this flow analysis may be stated as follows:

1. The fluid is a Newtonian, incompressible fluid.
2. The flow is two dimensional planar, turbulent.
3. Body forces are negligible.
4. Fluid velocity on the casing walls are zero

The coordinate system is chosen such that the origin of the Cartesian coordinate is at the center of the cross flow turbine rotor (blade and pipe).

Also, the boundary conditions of pressure:

At the inlet port: P_i = 981000 Pascal (Obtained from the entering water head)

At the outlet port: P_o = 101300 Pascal (the atmospheric pressure, since it is open)

Boundary conditions of temperatures:

At the inlet port: T_i = 20°c (considering ambient temperature)

At the outlet port: T_o = 25°c (assuming a minimum temperature increment due to the turbulence)

Pave type quadrilateral element is used for the grid creation of the finite element in Gambit.

5.2. Numerical Simulation

Computational fluid dynamics (CFD) performs numerical analysis of a fluid flow field once a finite volume grid has been created. Setting boundary conditions, defining fluid properties, executing the solution, refining the grid, and viewing and post processing the results are generally performed within the chosen CFD code.

2D numerical model of cross flow turbine drawn in solid works 2012 package

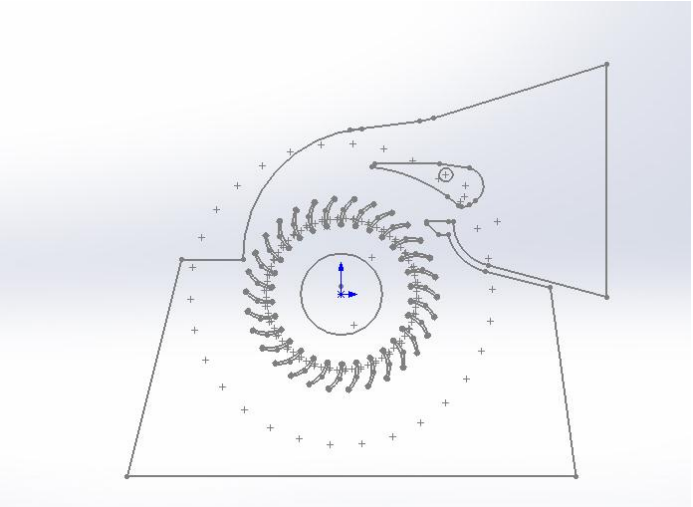

Figure 10:- A 2D sketch of the assembled model with the eccentric pipe

For this research, Solid Works is used for model construction, GAMBIT is used for preprocessing & grid generation, and FLUENT is used for the CFD solver.

5.2.1 GAMBIT, the Preprocessor for Geometry Modeling and Mesh Generation, Postprocessor for Results Viewing

GAMBIT is a software package designed to build, import and mesh models for computational fluid dynamics (CFD) and other scientific applications. GAMBIT gets user input by graphical user interface (GUI). Then the GUI performs the fundamental steps of building, meshing, and creating zone types in a model. The most important operations are associated with the Geometry, Mesh, Zones, and Exporting files for Postprocessing command buttons, which will be described here.

(i) Creating Geometry in Solid Works and importing it into GAMBIT

File -> Import -> IGES . The files were imported from Solid Works source files.

(ii) Meshing of the Model

Mesh command button on the Operation tool pad in GAMBIT opens the Mesh sub pad which contains command buttons that performs mesh operations involving boundary layers, edges, faces, volumes, and groups. In the particular problem of 2D cross flow model, this was used for face meshing

(iii) Specifying Zone Types

The domains of the model at its boundaries and in some specific regions can be defined by using zone-type specifications. There are two classes of zone-type specifications:

- Boundary types: Wall for rotor, guide valve and casing; Pressure Inlet for the inlet and Pressure Outlet for the outlet.
- Continuum types: Fluid for the meshed face.

(iv) Exporting Result Files from GAMBIT

To display post processing results for any given solution, two files must be imported into GAMBIT:

- A results database
- A neutral file

The results-database file contains the results data for the solution. The neutral file contains coordinate and connectivity information for the model.

5.2.2: FLUENT, the CFD Solver

FLUENT is a finite volume based code for the simulations and modeling of fluid flow as well as heat transfer. Since FLUENT is written in the C computer language, it makes full use of the flexibility and power offered by the language. FLUENT is ideally appropriate for incompressible and compressible fluid flow simulations in complex geometries.

Problem Solving Steps

Once after determining the important features of the particular problem of cross flow turbine, the following basic procedural steps were taken.

Geometrical Modeling and Meshing (in **Solid Works and GAMBIT)**

1. Create the model, the geometry and grid.

Preprocessing (in FLUENT)

2. Start the appropriate solver of FLUENT **for 2ddp** modeling.
3. Import the grid: **File** Menu
4. Check the grid: **Grid** Menu
5. Select the solver formulation: **Define** Menu
6. Choose the basic equations: laminar or turbulent (or inviscid) etc.: **Define** Menu
7. Specify material properties: **Define** Menu

Dynamic Mesh Zones: Moving Dynamic Mesh

8. Specify dynamic mesh zones & boundary conditions: **Define** Menu
9. Adjust the solution control parameters: **Solve** Menu
10. Initialize the flow field: **Solve** Menu

Calculation:

11. Calculate a solution: **Solve** Menu
12. Examine the results: **Display, Plot,** and **Report** Menu

Postprocessing:

13. Save the results: **File** Menu

Thus showing the numerical steps by using a logic diagram as shown below

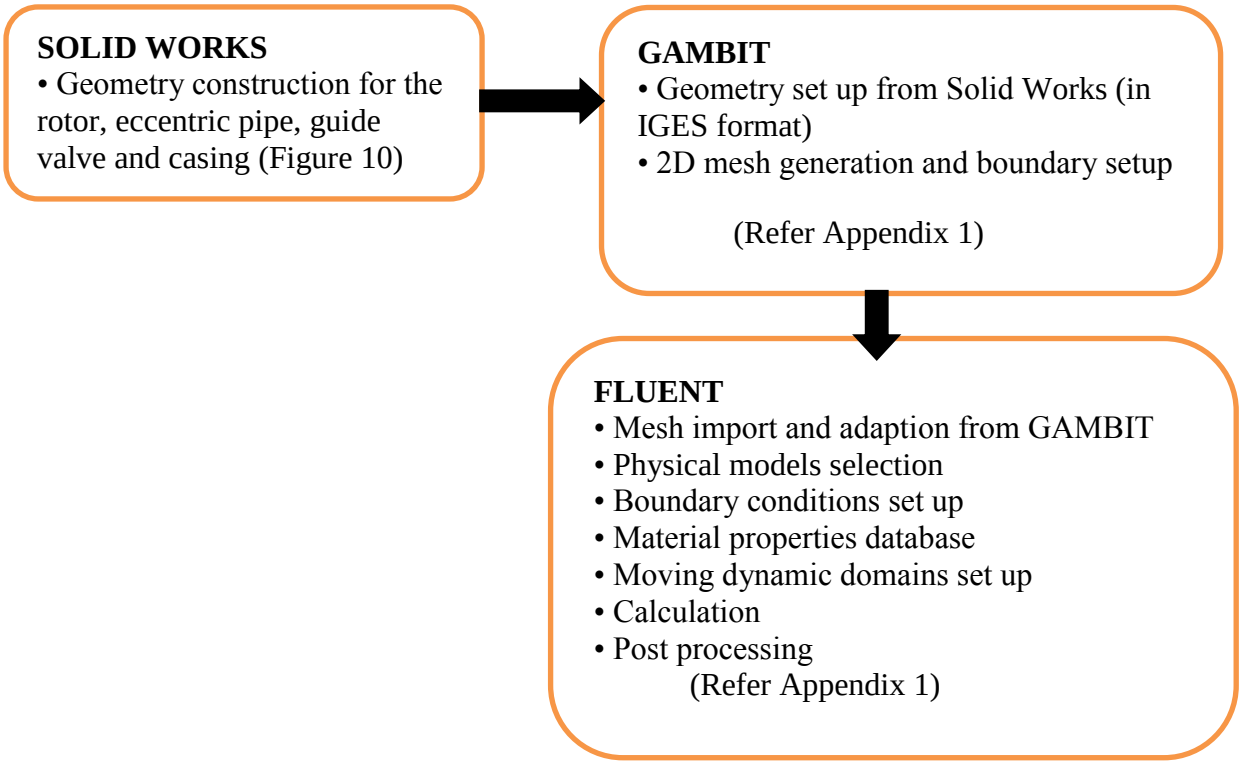

Chapter six: Results and interpretation

6.1: Results

In this section Contours of static pressure, dynamic pressure, velocity magnitude, radial velocity and velocity vectors colored by static pressure from the numerical analysis result of fluent for various eccentric pipe and guide valve position are shown clearly and their maximum and minimum range values are indicated as tabulated values.

6.1.1: Contours of static pressure

The following three figures shown below show the static pressure contours of models with four different eccentric pipe diameters at three different valve positions.

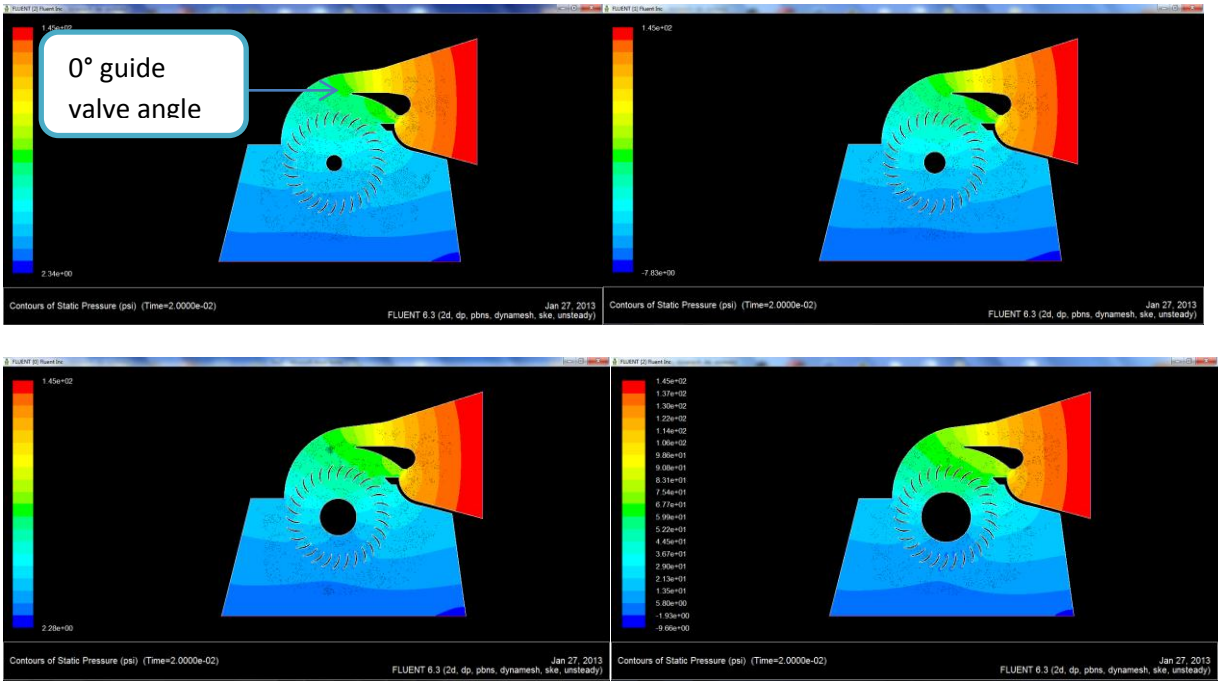

Fig 11: Contours of static pressure at guide valve angle of 0° from negative x-axis and eccentric pipe diameter of 45, 60, 100 and 135 with P_{in} =142.3 psi P_{out}=14.7psi, radial velocity(ω) =1.3 rad/s

The four contour diagrams shown in **Figure 11**, indicates the static pressure patterns inside the fluid interior at each point of fluid position with a varying eccentric pipe diameter but a similar guide vane angle position of 0°. As the fluid color goes from red to deep blue, the static pressure

magnitude goes from the maximum to the minimum (values are found in table 2, page 36). Fluid positions under a similar color contour means; it has an equal pressure magnitude. As it is seen from figure 11 above the light green color, at the fluid leaving the guide valve increases its coverage area as the eccentric diameter increases with the same with other parameters fixed constant for all of them.

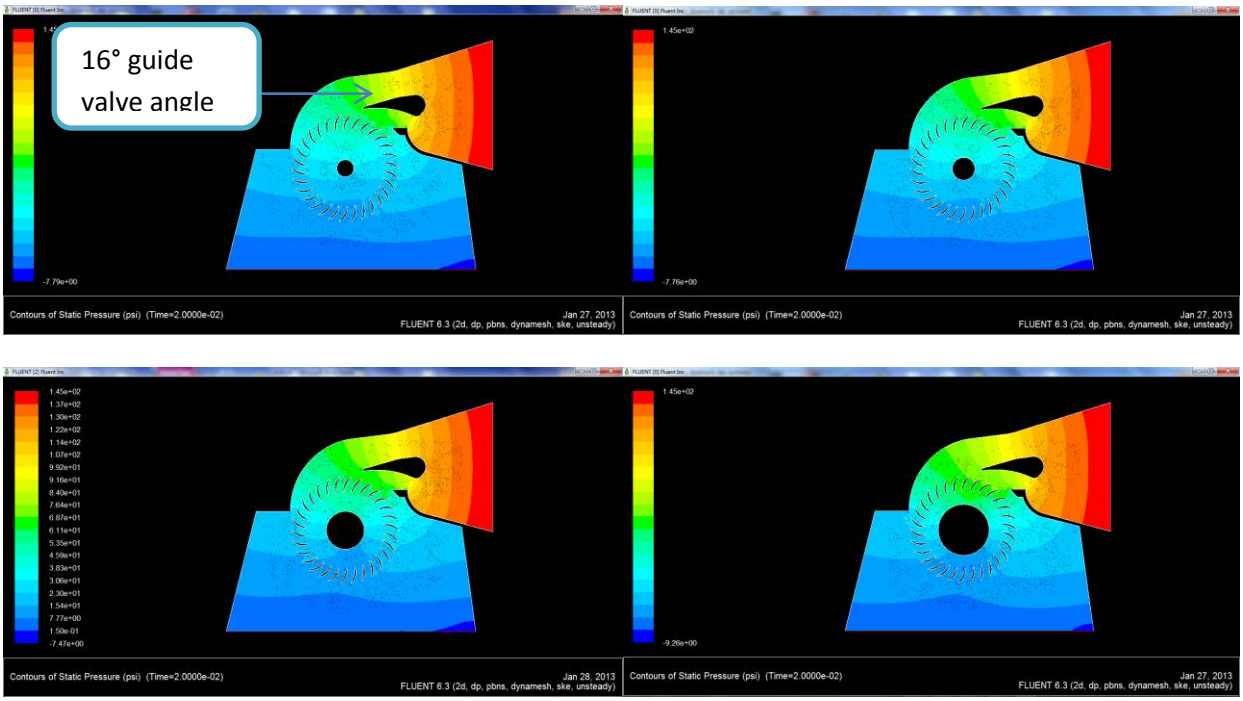

Fig 12: Contours of static pressure at guide valve angle of 16° from negative x-axis and eccentric pipe diameter of 45, 60, 100 and 135 with P_{in} =142.3 psi P_{out}=14.7psi, radial velocity(ω) =1.3 rad/s

Similarly the four contour diagrams in **Figure 12,** indicates the static pressure inside the fluid interior at each point of fluid position with a varying eccentric pipe diameter but a similar guide vane angle position of 16°. As the fluid color goes from red to deep blue, the static pressure magnitude goes from the maximum to the minimum (values are found in table 2, page 36). Similar to the case above, with valve angle of 0°, the light green colored fluid leaving the guide valve or (entering the 1st stage of energy conversion) increases its coverage as the diameter of the eccentric pipe increases. This static pressure contours unlike the contour at 0°, gives a decrease in a static pressure ranges.

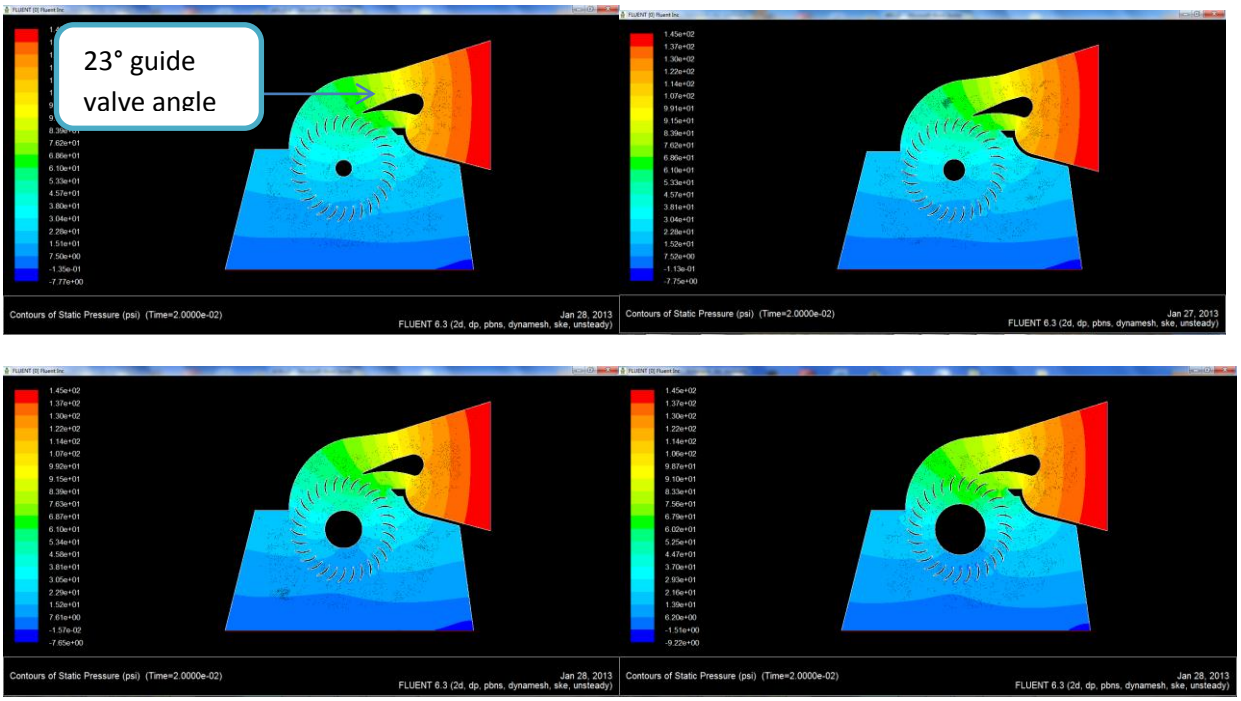

Fig 13: Contours of static pressure at guide valve angle of 23° from negative x-axis and eccentric pipe diameter of 45, 60, 100 and 135 with P_{in} =142.3 psi P_{out}=14.7psi, radial velocity(ω) =1.3 rad/s

As the two cases above these four contour diagrams in **figure 13** indicates the static pressure inside the fluid interior at each point of fluid position with a varying eccentric pipe diameter but a similar guide vane angle position of 23°. In here also as the fluid color goes from red to deep blue, the static pressure magnitude goes from the maximum to the minimum values (the values are found in table 2, page 36). The fluid pattern seen in these contour diagrams, like the above other cases, shows an increase better pressure fluid area at the first entrance outer periphery of the rotor. This static pressure contours unlike the contour at 0° and 16°, gives a decrease in maximum and minimum static pressure ranges. However the fluid pattern around the rotor gets lighter and lighter as the guide valve angle increases from 0° to 23°.

6.1.2: Contours of dynamic pressure

The following three figures shown below indicates the dynamic pressure contour diagram results of fluent for eccentric pipe diameters of 45, 60, 100, and 135mm at three different guide valve angle positions, which are 0°, 16°, and 23°. Fluid patterns under a similar color means, it has an equal dynamic pressure magnitude.

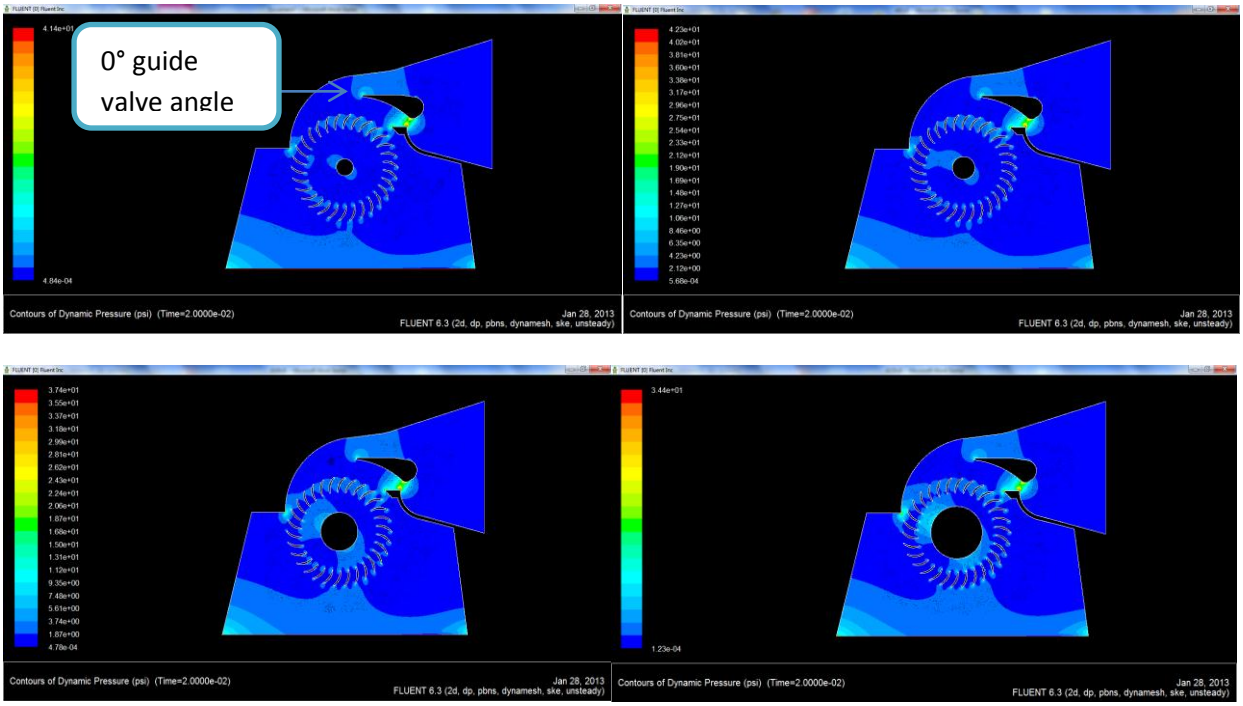

Fig 14: Contours of dynamic pressure at guide valve angle of 0° from negative x-axis and eccentric pipe diameter of 45, 60, 100 and 135 with P_{in} =142.3 psi P_{out}=14.7psi, radial velocity(ω) =1.3 rad/s

The dynamic pressure contour diagrams above, **figure 14**, indicates the dynamic pressure values inside the fluid interior at each point of fluid position with a varying eccentric pipe diameter but a similar guide vane angle position of 0°. As the fluid color goes from red to deep blue, the dynamic pressure magnitude goes from the maximum to minimum value (these values are found in table 3, page 36). From the figure it is found that as the eccentric pipe diameter increases a fluid with a greater dynamic pressure magnitude appears around the eccentric pipe, where the fluid exits the first stage and enters the second stage.

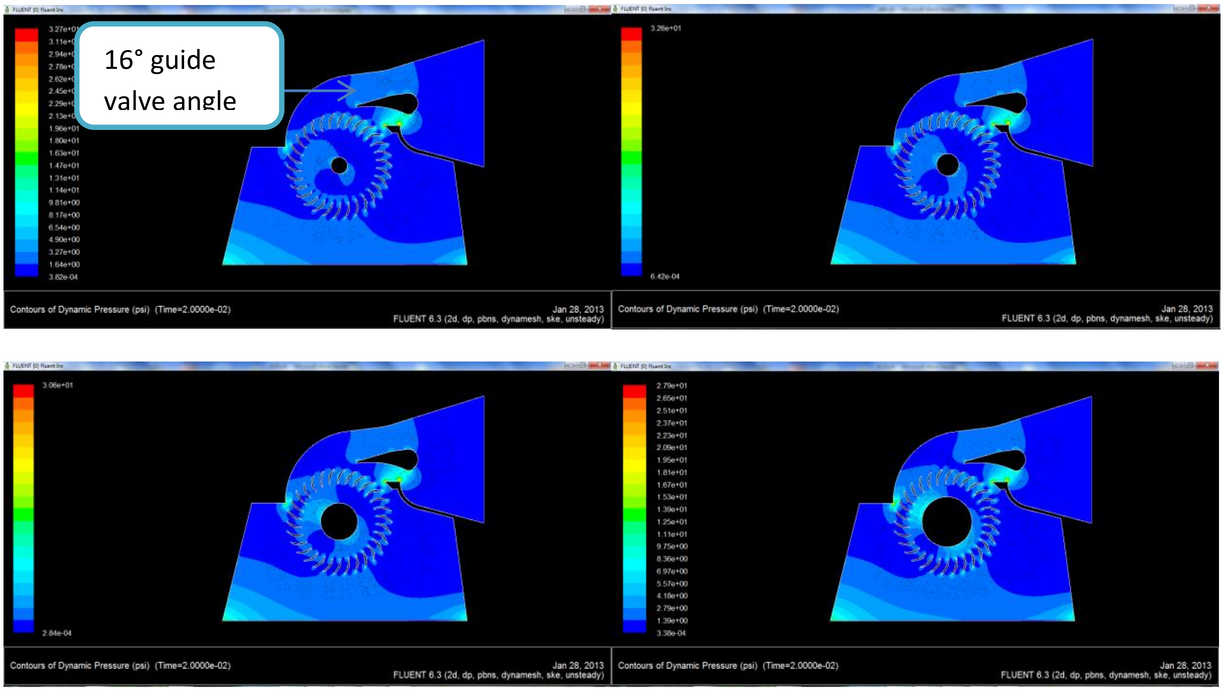

Fig 15: Contours of dynamic pressure at guide valve angle of 16° from negative x-axis and eccentric pipe diameter of 45, 60, 100 and 135 with P_{in} =142.3 psi P_{out}=14.7psi, radial velocity(ω) =1.3 rad/s

In the second dynamic pressure contour diagrams above, **figure 15**, it indicates the dynamic pressure values inside the fluid interior at each point of fluid position with a varying eccentric pipe diameter but a similar guide vane angle position of 16°. Similar to the figure 14, in these figures as the fluid color goes from red to deep blue, the dynamic pressure magnitude goes from the maximum to minimum value (these values are found in table 3, page 36). In this figure it is also found that as the eccentric pipe diameter increases a fluid with a greater dynamic pressure magnitude appears around the eccentric pipe, where the fluid exits the first stage and enters the second stage but the patterns coverage areas are wider than the ones seen for the case of dynamic pressure contours at guide valve angle of 0°.

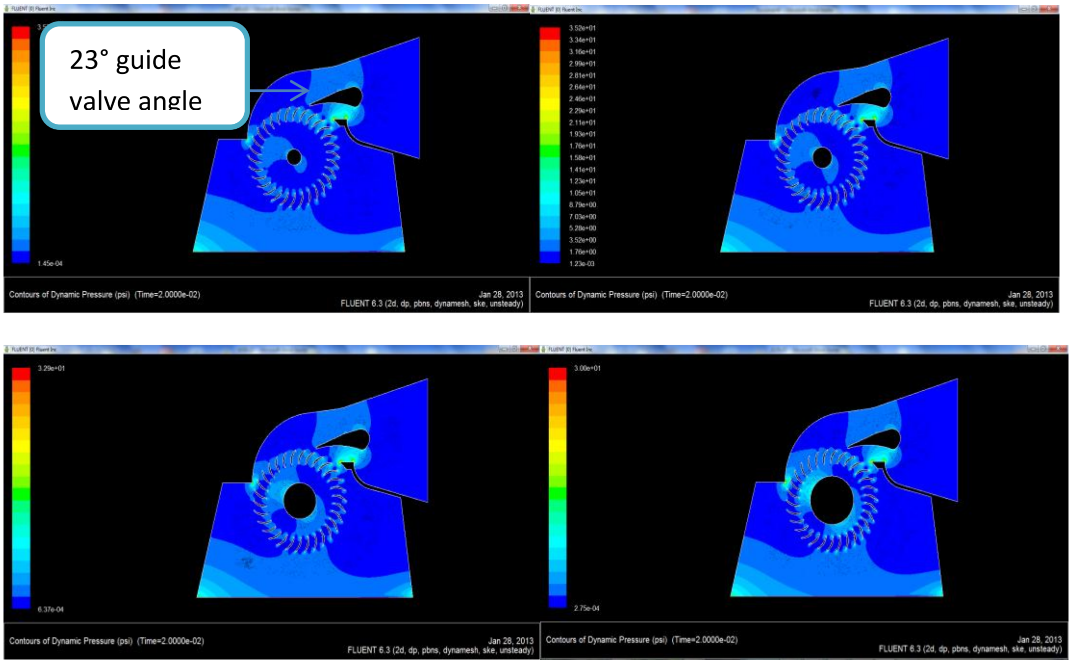

Fig 16: Contours of dynamic pressure at guide valve angle of 23° from negative x-axis and eccentric pipe diameter of 45, 60, 100 and 135 with P_{in} =142.3 psi P_{out}=14.7psi, radial velocity(ω) =1.3 rad/s

These dynamic pressure contour diagrams, **figure 16**, like the other two above indicates the dynamic pressure values inside the fluid interior at each point of fluid position with a varying eccentric pipe diameter but a similar guide vane angle position of 23°. In a Similar way like the other two figures, in these figures the dynamic pressure magnitude goes from maximum to minimum values as the fluid color goes from red to deep blue (these values are found in table 3, page 36). These maximum and minimum range values seen to show a decrease in their magnitude as the eccentric pipe diameter increases from 45mm to 1000mm. Also found that as the eccentric pipe diameter increases a fluid with a greater dynamic pressure magnitude appears around the eccentric pipe, where the fluid exits the first stage and enters the second stage but the patterns coverage areas are wider than the ones seen for the cases of dynamic pressure contours at guide valve angle of 0° and 16°.

6.1.3: Contours of velocity magnitude

The contour diagrams in this section are diagrams that show the velocity magnitude contours for four different eccentric pipe diameter cases (45, 60, 100, and 135mm) at three different guide valve angle positions (0°, 16°, and 23°).

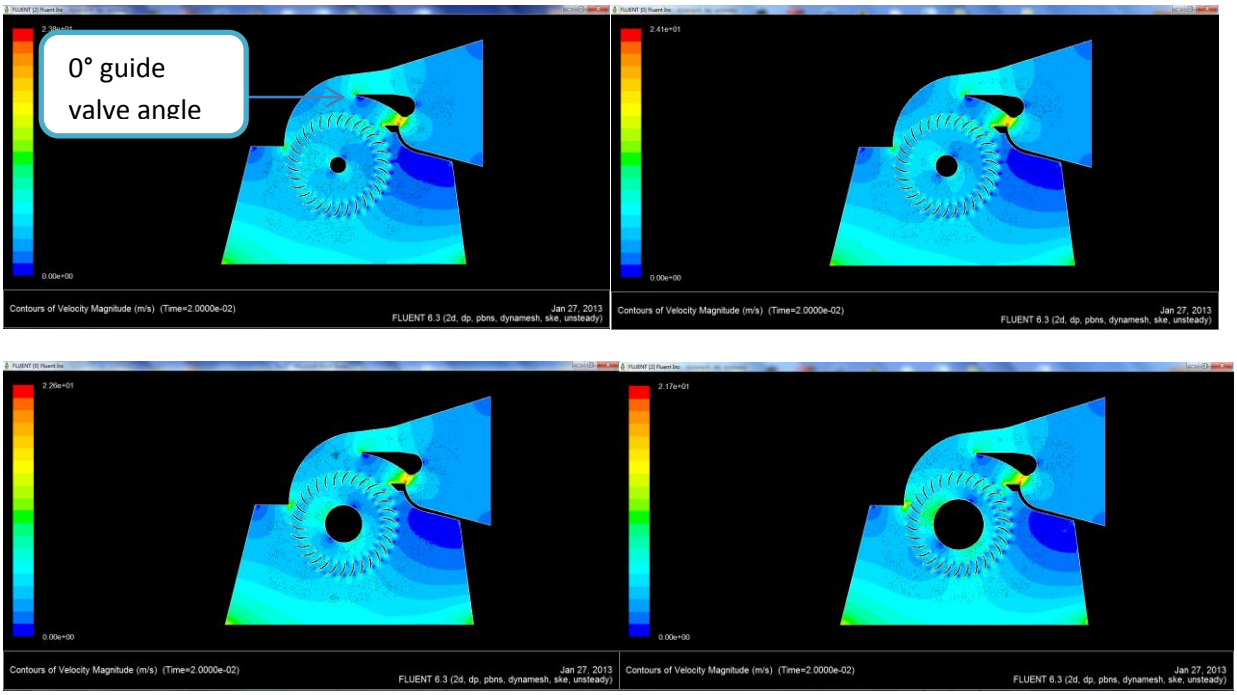

Fig 17: Contours of velocity magnitude at guide valve angle of 0° from negative x-axis for different eccentric pipe diameter (45, 60, 100 and 135mm) with P_{in} =142.3 psi, P_{out}=14.7psi, radial velocity(ω) =1.3 rad/s

The term velocity magnitude defines the resultant velocity magnitude of fluid particles at any position. The diagrams in **Figure 17** describes the velocity contour diagrams results obtained from fluent numerical analysis for varying eccentric pipe diameter but a similar guide valve angle position of 0°. As the bar in front of each diagram shows the magnitude of velocity in the contour increases with the color goes from deep blue to red. The maximum and minimum values are indicated in table 4 page 37. Keeping the other flow and physical parameters constant except the pipe diameter for all cases, a velocity pattern area with a better velocity magnitude wide up as the diameter of eccentric pipe goes from 45 to 135mm. But the maximum velocity range decreases while pipe diameter increases. The minimum value remains constant for all cases.

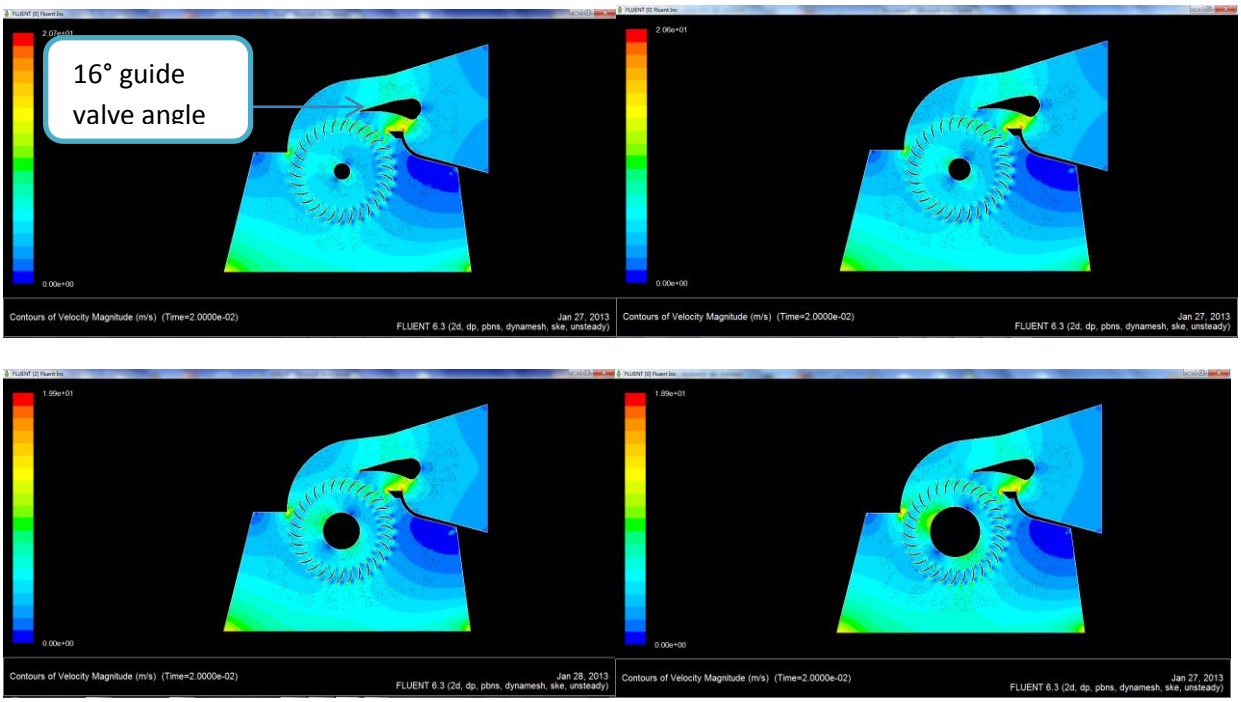

Fig 18: Contours of velocity magnitude at guide valve angle of 16° from negative x-axis for different eccentric pipe diameter (45, 60, 100 and 135mm) with P_{in} =142.3 psi, P_{out}=14.7psi, radial velocity(ω) =1.3 rad/s

In **Figure 18,** contour diagrams of the cross flow turbine under consideration describes the velocity contour diagrams results obtained from fluent numerical analysis for varying eccentric pipe diameter but a similar guide valve angle position of 16°. The color variation from deep blue to red in the contour corresponds to a velocity magnitude variation from maximum to minimum values. In these contour diagrams like the one with guide valve angle an angle of 0°, show an increment pattern coverage area of fluid with a greater velocity around the eccentric pipe first stage exit and second stage entrance locations as the diameter of the pipe increases from 45mm to 135mm. But the maximum range value decreases with increasing pipe diameter.

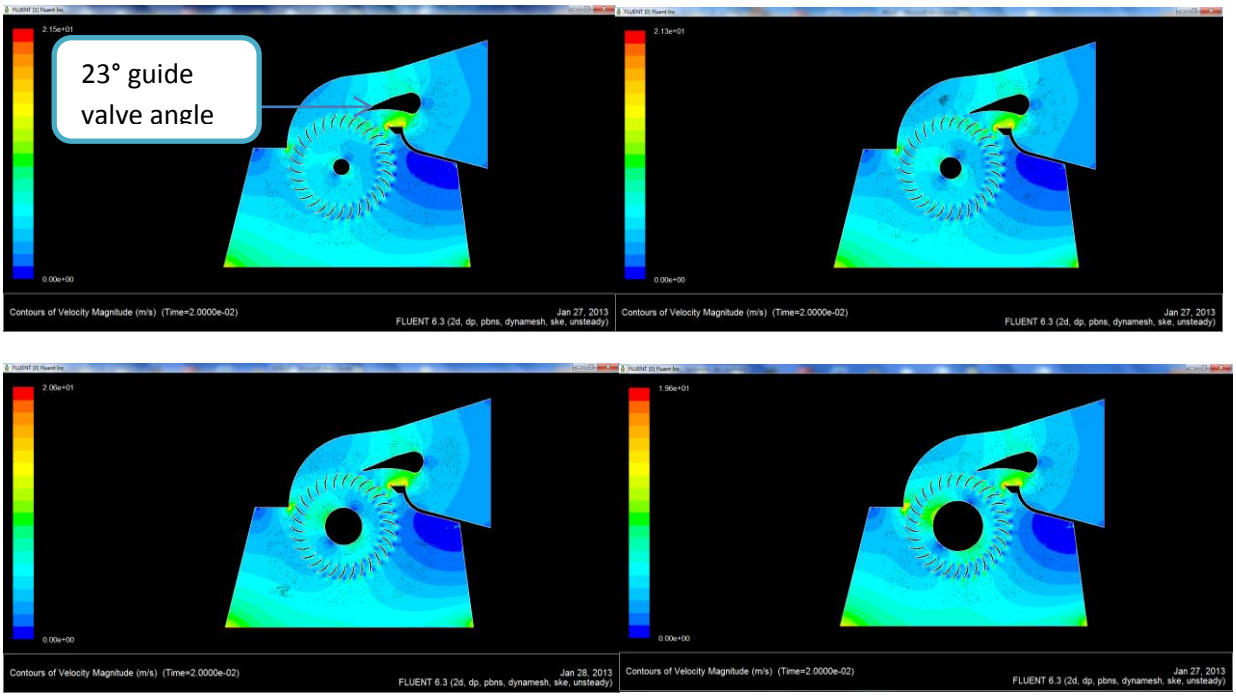

Fig 19: Contours of velocity magnitude at guide valve angle of 23° from negative x-axis for different eccentric pipe diameter (45, 60, 100 and 135mm) with P_{in} =142.3 psi, P_{out}=14.7psi, radial velocity(ω) =1.3 rad/s

The velocity contour diagrams shown in **Figure 19** indicates velocity contour diagram results obtained from fluent numerical analysis for varying eccentric pipe diameter but a similar guide valve angle position of 23°. Like the other two figures the velocity magnitude goes from maximum to minimum as the color goes from red to deep blue. Again as the diameter of the eccentric pipe increases the increased velocity pattern area widen up around the eccentric pipe at the 1st stage exit and entrance to the second stage similar to the above two cases of guide valve angle of 0°, and 16°. Also the maximum velocity range value decreases with increasing the pipe diameter. Besides showing colored velocity magnitude patterns of interior fluid these contour diagrams gives the maximum and minimum value ranges of velocity magnitude obtained. These values are tabulated in table 4, of page 37.

6.1.4: Velocity vector colored by static pressure

The following figures below shows zoomed and normal diagrams of a velocity vector colored by static pressure resulted from the simulation analysis for four different eccentric pipe diameter at three guide valve angle position.

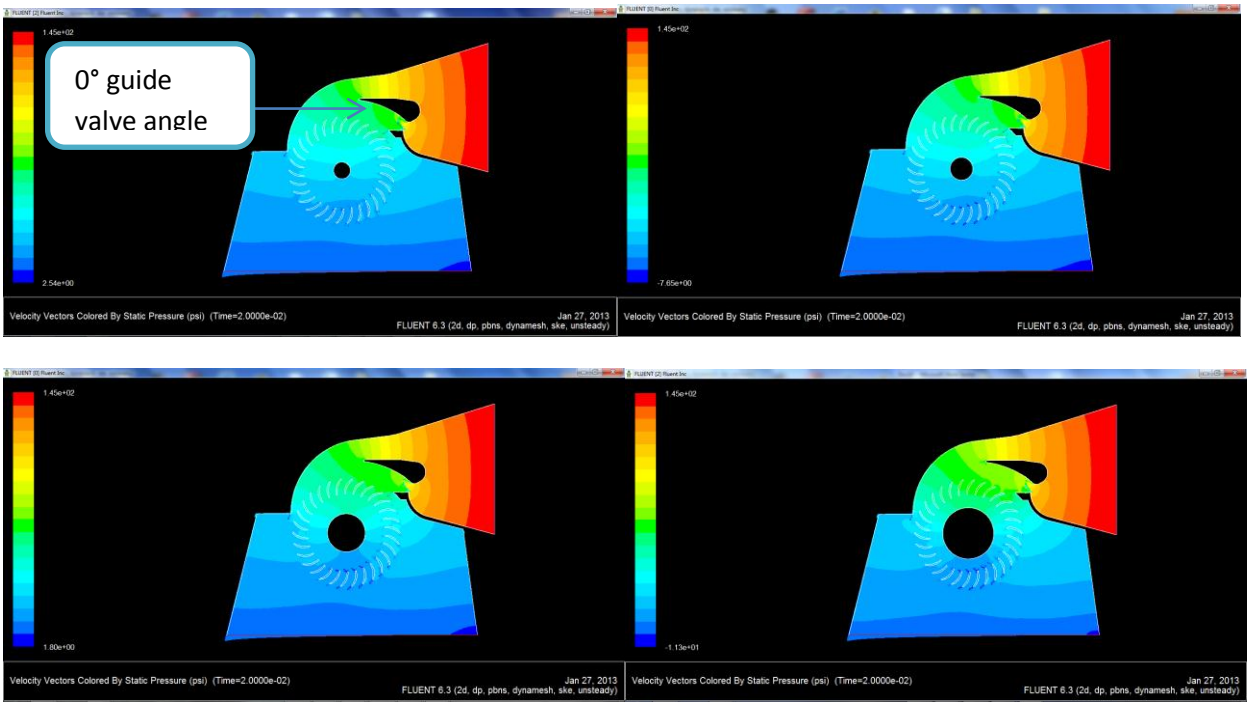

Fig 20: Velocity vector colored by static pressure at guide valve angle of 0° from negative x-axis for different eccentric pipe diameter (45, 60, 100 and 135 mm)with P_{in} =142.3 psi, P_{out}=14.7psi, radial velocity(ω) =1.3 rad/s

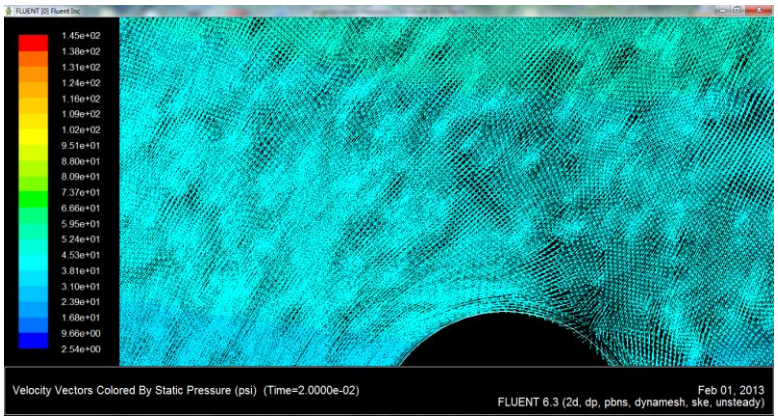

From **figure 21** we can see that the eccentric pipe is diverting the direction of the fluid passing by it.

Fig 21: Zoomed in velocity vector colored by static pressure of D45v0

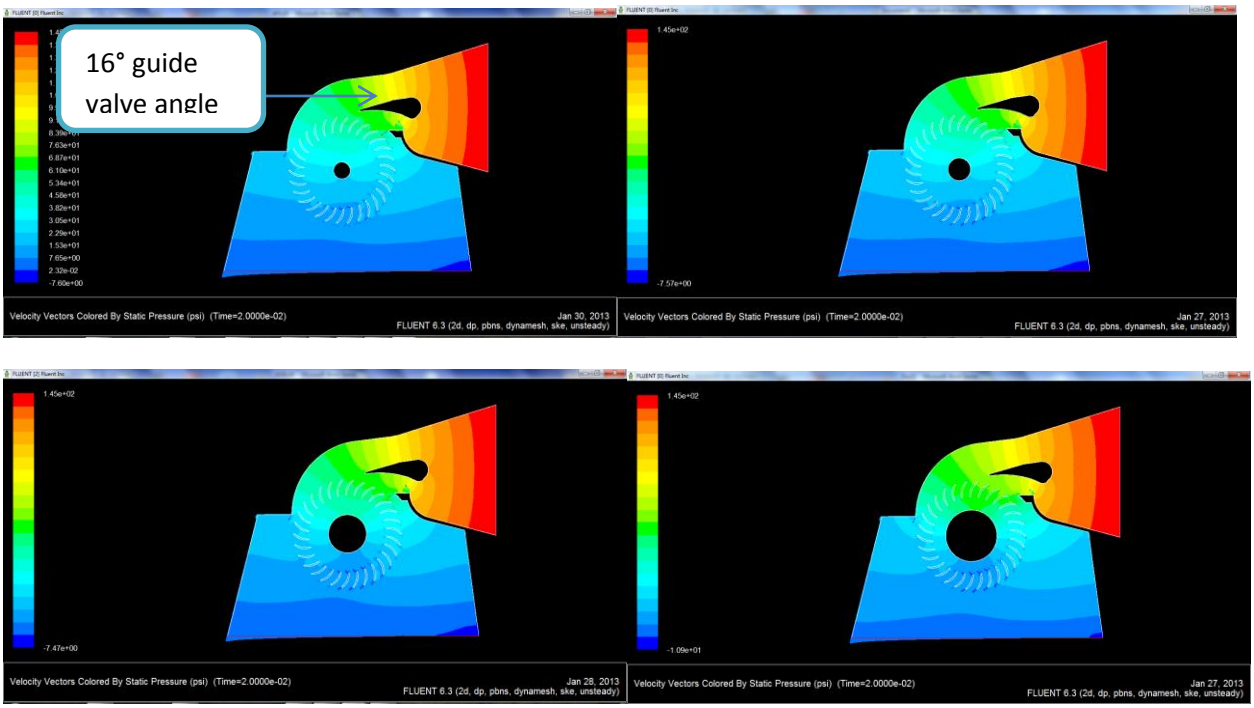

Fig 22: Velocity vector colored by static pressure at guide valve angle of 0° from negative x-axis for different eccentric pipe diameter (45, 60, 100 and 135 mm)with P_{in} =142.3 psi, P_{out}=14.7psi, radial velocity (ω) =1.3 rad/s

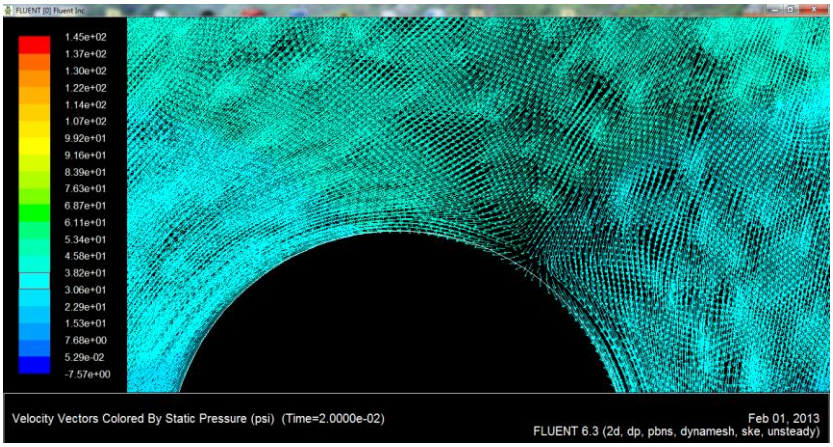

Fig 23: Zoomed in velocity vector colored by static pressure of D60v16

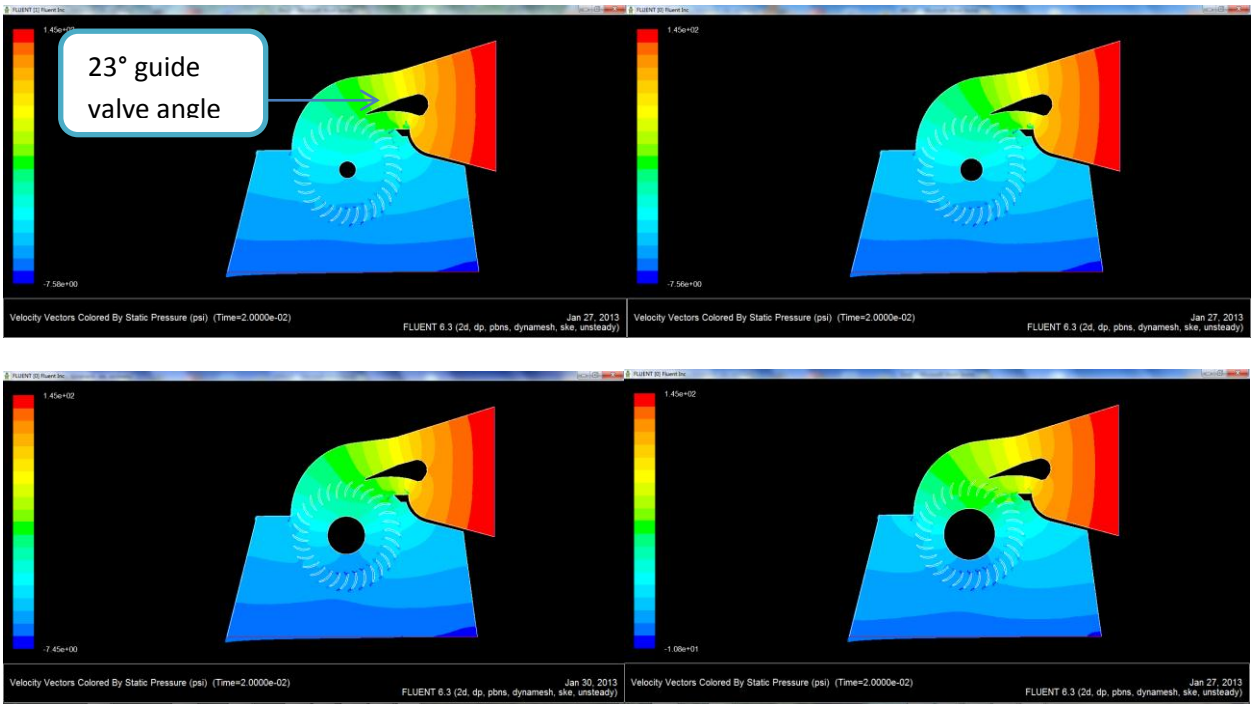

Fig 24: Velocity vector colored by static pressure at guide valve angle of 0° from negative x-axis for different eccentric pipe diameter (45, 60, 100 and 135 mm)with P_{in} =142.3 psi, P_{out}=14.7psi, radial velocity(ω) =1.3 rad/s

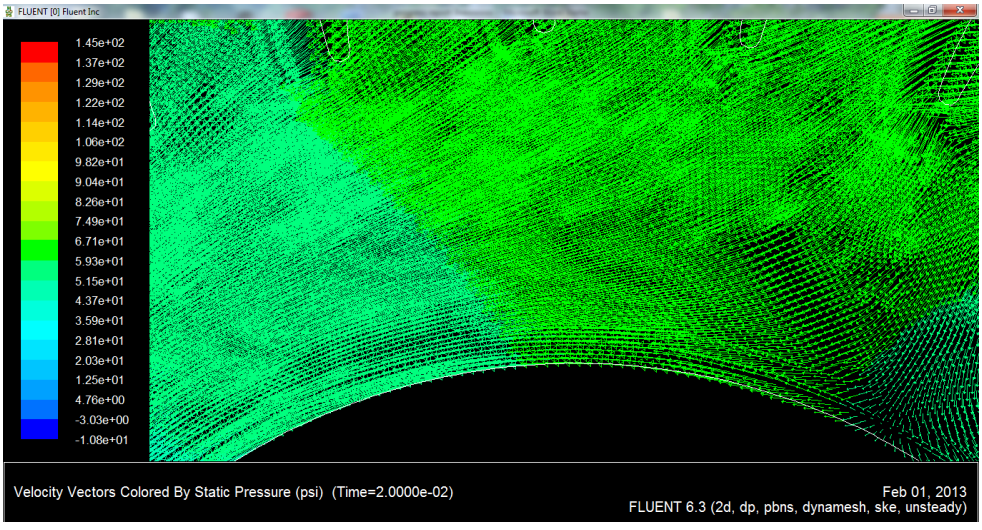

Fig 25: Zoomed in velocity vector colored by static pressure of D135v23

6.1.5: Table from the numerical analysis results that shows velocity and pressure ranges

The following values in the table are the results of the numerical analysis which shows the minimum and maximum ranges of the static pressure, dynamic pressure, velocity magnitude and radial velocity found from the corresponding contours. As noted on page 44, the velocity and the pressure distributions shown in the figures must be reduced by the geometric scaling factor (appendix 1, page 44-grid).

Table 2: Static pressure range at different guide valve angle and eccentric pipe diameter with the same flow parameters of P_{in} =142.3 psi P_{out}=14.7psi, radial velocity (ω) =1.3 rad/s

Eccentric pipe diam.	static pressure range at guide valve angle of 0° (min - max)		static pressure range at guide valve angle of 16° (min - max)		static pressure range at guide valve angle of 23° (min - max)	
45	2.344749	144.9606	-7.663983	144.9556	-7.771	144.9484
60	-7.83238	144.9595	-7.791858	144.9511	-7.74751	144.9493
100	2.282997	144.9638	-7.764043	144.952	-7.645595	144.9532
135	-9.662968	144.9661	-9.262421	144.9606	-9.222327	144.9585

Table 3: Dynamic pressure at different guide valve angle and eccentric pipe diameter with the same flow parameters of P_{in} =142.3 psi P_{out}=14.7psi, radial velocity (ω) =1.3 rad/s

Eccentric pipe diam.	Dynamic pressure range at guide valve angle of 0° (min - max)		Dynamic pressure range at guide valve angle of 16° (min - max)		Dynamic pressure range at guide valve angle of 23° (min - max)	
45	0.0004835851	41.39926	0.0003817047	32.69454	0.0001446098	35.74783
60	0.0005677612	42.3084	0.00064248	32.62158	0.001225742	35.16187
100	0.0004778304	37.40049	0.0002844408	30.61024	0.0006370042	32.88385
135	0.0001232829	34.39003	0.0003377694	27.86059	0.0002753117	30.00254

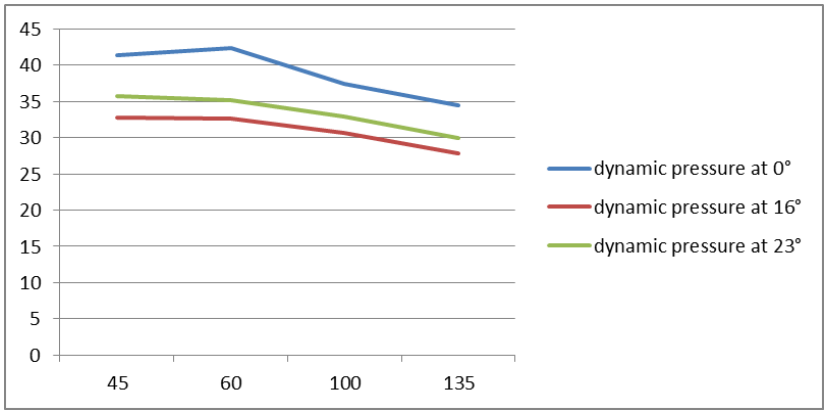

Fig 26: maximum values of dynamic pressure

Table 4: Velocity magnitude ranges at different guide valve angle and eccentric pipe diameter with the same flow parameters of P_{in} =142.3 psi P_{out}=14.7psi, radial velocity (ω) =1.3 rad/s

Eccentric pipe diam	Velocity magnitude range at an angle of 0°		Velocity magnitude range at an angle of 16°		Velocity magnitude range at an angle of 23°	
45	0	23.83178	0	20.73746	0	21.50926
60	0	24.09029	0	20.62503	0	21.32075
100	0	22.64622	0	19.89373	0	20.6072
135	0	21.71133	0	18.93653	0	19.59291

Table 5: Radial velocity ranges at different guide valve angle and eccentric pipe diameter with the same flow parameters of P_{in} =142.3 psi P_{out}=14.7psi, radial velocity (ω) =1.3 rad/s.

Eccentric pipe diam.	radial velocity range at guide valve angle of 0° (min - max)		radial velocity range at guide valve angle of 16° (min - max)		radial velocity range at guide valve angle of 23° (min - max)	
45	-17.86086	11.27847	-19.7126	11.31926	-20.56062	11.32501
60	-18.26706	11.27639	-19.72976	11.30509	-20.43028	11.30923
100	-17.33711	11.20144	-19.11995	11.23752	-19.0219	11.24031
135	-17.04282	11.11602	-18.3322	11.13792	-18.9663	11.13948

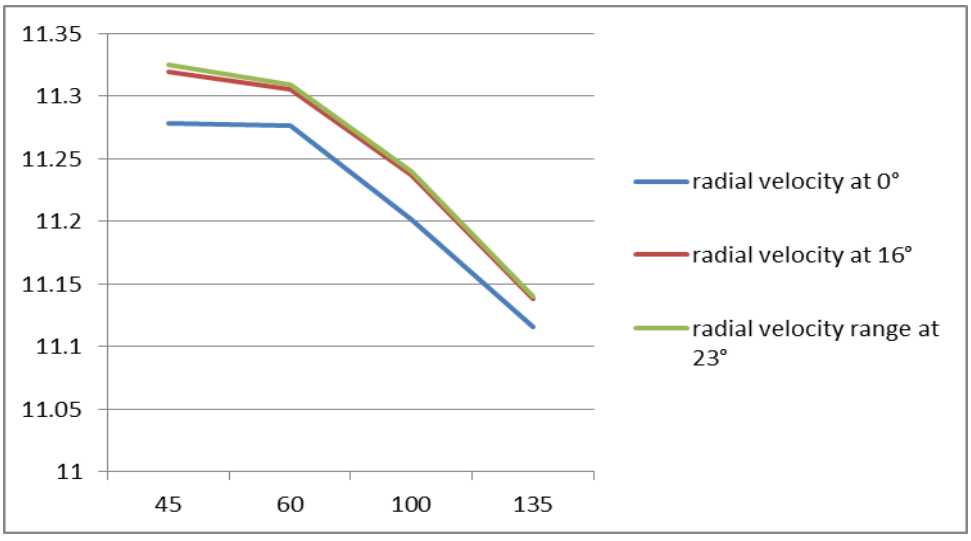

Fig 27: the maximum range values of radial velocity

6.2: Values from numerical analysis result that show Pressure, viscous and total moments on bade and pipe at different eccentric pipe diameter and guide valve position

The following tables and graphs show values of pressure, viscous and total moment on the rotor part of the turbine obtained from the simulation of the models at different eccentric pipe diameter and guide valve angle position. Keep in mind that since the negative sign of the values show only the direction of moment, the moment Vs eccentric diameter graph uses the magnitude of the values.

Blade-and-pipe of model	Pressure moment (about z-axis) N-m	viscous moment (about z-axis)Nm	total moment (about z-axis) N-m
D45v0	-961069.28	-2455.87	-963525.16
D60v0	-893691.79	-2848.2	-896539.99
D100v0	-941199.01	-3005.02	-944204.03
D135v0	-1017670.6	-3400.47	-1021071.1

Table 6: pressure, viscous and total moment on blade and pipe at 0° guide valve position

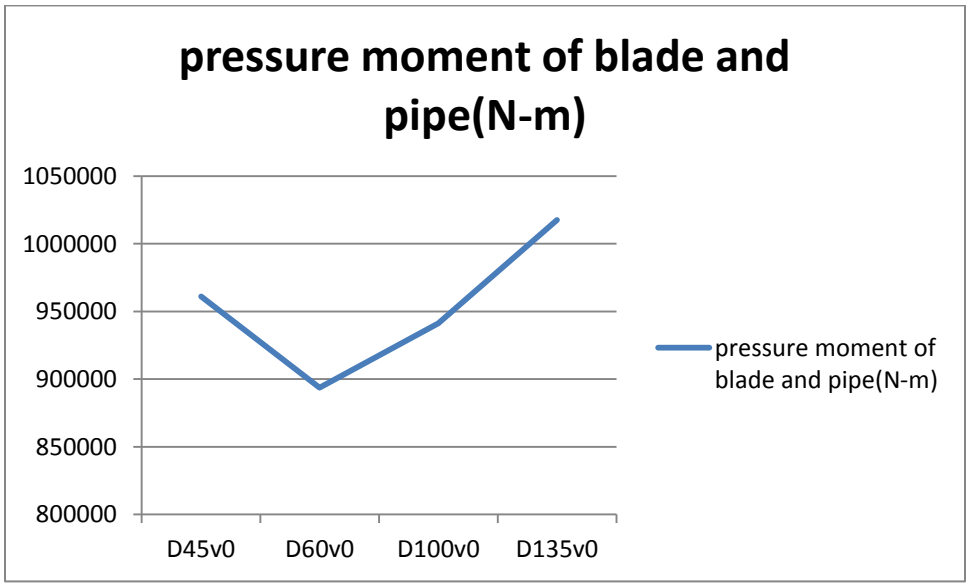

Fig 28: pressure moment of blade and pipe Vs eccentric pipe diameter at 0° valve angle

Blade-and-pipe of model	Pressure moment (about z-axis) N-m	viscous moment (about z-axis)Nm	total moment (about z-axis) N-m
D45v16	-944687.86	-2725.93	-947413.8
D60v16	-913882.86	-2870.09	-916752.95
D100v16	-965491.51	-3040.05	-968531.56
D135v16	-1040885	-3434.3	-1044319.3

Table 7: pressure, viscous and total moment on blade and pipe at 16° guide valve position

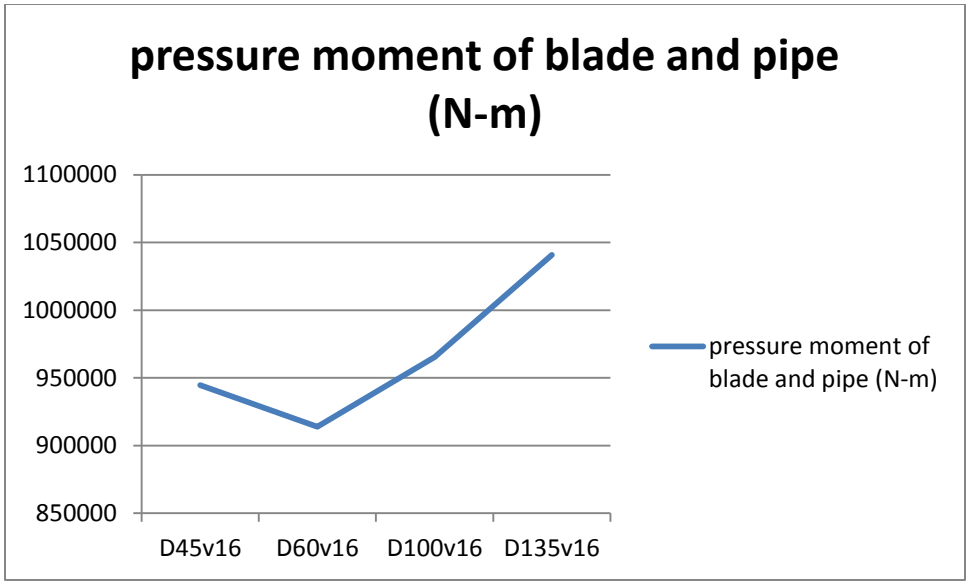

Fig 29: pressure moment of blade and pipe Vs eccentric pipe diameter at 16° valve angle

Blade-and-pipe of model	Pressure moment (about z-axis) N-m	viscous moment (about z-axis)Nm	total moment (about z-axis) N-m
D45v23	-911762.7	-2859.97	-914622.65
D60v23	-923585.77	-2872.23	-926458
D100v23	-974077.57	-3041.45	-977119.02
D135v23	-1051517.8	-3442.7	-1054960.5

Table 8: pressure, viscous and total moment on blade and pipe at 23° guide valve position

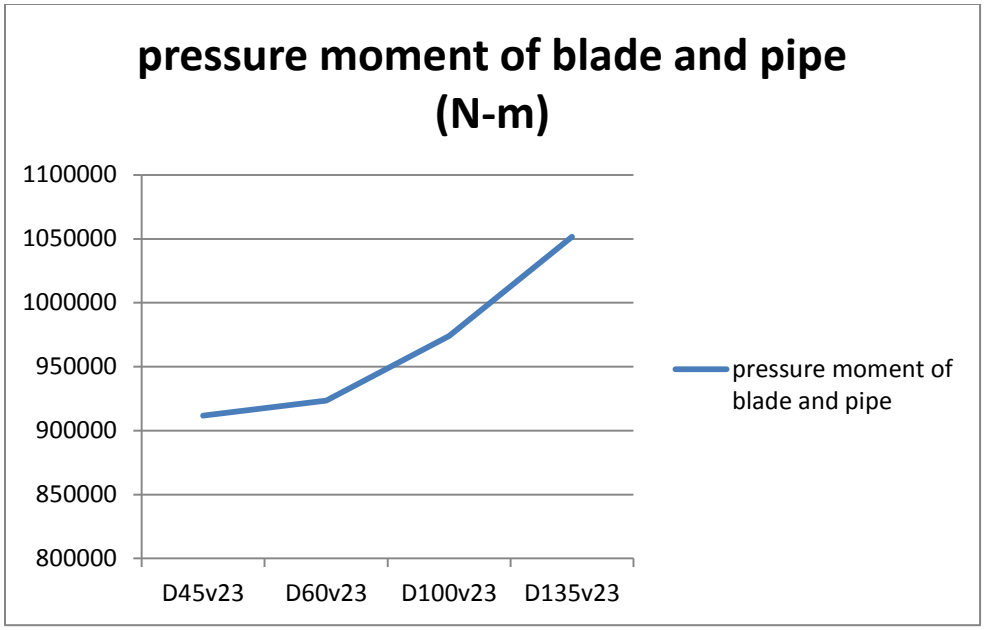

Fig 30: pressure moment of blade and pipe Vs eccentric pipe diameter at 23° valve angle

6.3: Interpretation of the result

The static pressure ranges obtained from the numerical analysis for a guide valve angle position of 0° show a non-uniform variation that needs additional sample models to exactly interpret the effect of the eccentric pipe variation. While on the other guide valve angle positions it shows a decrease in minimum static pressure as increasing the eccentric pipe diameter though the variation is very small. For all guide valve angle positions the maximum static pressure remains almost constant showing a non-considerable change with increasing the diameter of the eccentric pipe.

When we see the dynamic pressure range values, regardless of unexpected results on the 60 mm diameter pipe, which shows increase in the minimum dynamic pressure, all others show a decrease in minimum velocity with increasing pipe diameter for all guide valve positions. Unlike the static pressure ranges the maximum dynamic pressure shows a decrease in its magnitude with increasing pipe diameter for all guide valve angle position except for 0° guide angle position.

In the case of velocity magnitude range the minimum velocity is zero for all cases, the only variation is shown on the maximum velocity magnitude. The maximum velocity range shows a

decrease in magnitude with increasing pipe diameter except for 60mm diameter at 0° guide valve position.

The numerical analysis result shows that the radial velocity range of the fluid interior decreases with increasing eccentric pipe diameter for all guide valve angle position but all values tends to increase with increasing guide valve angle from the horizontal negative x-axis regardless of the pipe diameter variation.

As the velocity vector results colored by static pressure (as shown on figs 22-24) show the eccentric pipes has an effect of diverting the fluid direction as the fluid enters to the second stage of cross flow.

Considering the mechanical power obtained, since the above parameter only represent the energy in the fluid entering and leaving the turbine, the numerical analysis report, as shown in tables 6-8 and the graphs on fig 25-27, that the pressure moment on the rotor (blade and pipe) increases with increasing the eccentric pipe diameter except for 60mm diameter pipe at 0° and 16°. Thus from rotational mechanical energy equation, for a given angular velocity increasing the torque increases the mechanical power.

Chapter seven: Conclusion and recommendation

7.1: Conclusion

As the interpretation of the analysis results indicates, increasing the eccentric pipe diameter will result in decreasing the limit of static and dynamic pressure ranges, velocity magnitudes and radial velocity of the fluid as obtained from the contours with some exceptions. This interpretation implies that the energy carried on by the entering fluid by any means losses its fluid power. Which means that the hydraulic energy is converted to some other energy form which in our case either to heat energy or mechanical energy.

Beside the hydraulic power loss stated, the other report of the numerical analysis shows an increasing in mechanical energy which in our case obtained from the fluid power entering the turbine.

Hence using an eccentric pipe at the center of a rotor in a cross flow turbine tend to decrease the fluid power and increase the mechanical power output from the rotor with increasing the pipe diameter for the given flow parameters of this thesis. Besides the eccentric pipe has the tendency to divert the flow direction of the fluid at the second stage as shown on the velocity vector diagrams of the simulation result.

Because the case study model numbers are not enough to indicate an optimum eccentric pipe range since our models didn't show expected fine results besides the numerical results has to be supported by experimental results it is unable to get optimum diameter values.

7.2: Recommendation

Increasing the number of models, with a small eccentric pipe diameter gape from each consecutive samples, for each guide valve position will give a fine solution which will clearly show the efficient eccentric pipe diameter range for the given flow parameter and others, which need a better simulation machine and extended time. Also needs to support it with experimental results.

The optimum eccentric pipe diameter range for a given flow parameters could be standardized by undergoing laboratory experiments as well.

As a future work a

- 3D simulation should be considered since it give a better view of numerical flow analysis as the 2D has a limitation in showing the actual and practical view unlike the 3D.
- Increasing the time step value in the iteration of the simulation, though it needs a better simulation machine and extended simulation time, it gives a good view of the flow.

References

[1] Water for agriculture and energy in Africa ministerial conference on water for agriculture and energy in africa: the challenges of climate change: Sirte, Libyan Arab Jamahiriya, 15-17 December 2008

[2] Hydropower of Ethiopia: Status, Potential and Prospects; By Solomon Seyoum Hailu (Former Manager, Medium Scale Hydropower Development Project) in 2007.

[3] Micro Hydro Power Resource Assessment Handbook Prepared for Asian and Pacific Centre for Transfer of Technology Of the United Nations – Economic and Social; Commission for Asia and the Pacific (ESCAP); By Dilip Singh; September 2009

[4] design of a cross flow turbine for a micro-hydro power application by Javed A. Chattha, Mohammad S. Khan, Syed T. Wasif, Osama A. Ghani, Mohammad O. Zia, Zohaib Hamid; Faculty of Mechanical Engineering; GIK Institute of Engineering Sciences & Technology; Topi, NWFP, Pakistan.

[5] The Banki Water Turbine, by proff. C.A. Mockmore civil engineer and proff. Fred Meryfield civil engineer, bulletin series No. 25 February 1949, engineering experiment station origon University.

[6] Performance and flow characteristics lattitude of nozzle in turbine blades second level; By Jusuf Haurissa, Rudy Soenoko; Department of Mechanical Engineering, University of Brawijaya Malang (INDONESIA)

[7] Numerical Investigation of the Internal Flow in a Banki Turbine By Jes´us De Andrade, Christian Curiel, Frank Kenyery, Orlando Aguill ´ on, Auristela V´asquez, andMiguel Asuaje; Laboratorio de Conversi´on de Energ´ıa Mec´anica, Universidad Sim´on Bol´ıvar, Valle de Sartenejas, Caracas 1080, Venezuela.

[8] Investigation of the performance of a cross-flow turbine by HAYATI OLGUN* ; Mechanical Engineering Department, Karadeniz Technical University, Trabzon 61080, Turkey

[9] Effect of interior guide tubes in cross-flow turbine runner on turbine performance by Hayati Olgun; Tubitak Marmara Research Center, Energy Systems and Environmental Research Institute, P.O. Box 21, Gebze 41470,Kocaeli, Turkey.

[10] Parametric Evaluation of Cross-Flow Turbine Performance J. Energy Eng. 120, 17 (1994); doi:10.1061/(ASCE)0733-9402(1994)120:1(17) (18 pages) ; by V. R. Desai and N. M. Aziz, Member, ASCE ; Visiting Asst. Prof., Dept. of Civ. Engrg., Clemson Univ., Clemson, SC 29634-0911 ; Assoc. Prof., Dept. of Civ. Engrg., Clemson Univ., Clemson, SC

[11] Influence of Solidity on the Performance of a Cross –Flow Turbine by C.A. Consul, R.H.J Willden, E. Ferrer, M.D. McCulloch Department of Engineering Science; University of Oxford; Parks Road, OX1 3PJ, Oxford, UK.

[12] Simulation and evaluation of a straight-bladed darrieus-type cross flow marine turbine by S Lain and C Osorio. Energetic and mechanics department, Fluid mechanics research group, Universidad Autonoma de occcidente, cali(colombia); December 2010.

[13] Fundamentals of Computational Fluid Dynamics, by Harvard Lomax and Thomas H.Pulliam NASA Ames Research Center, and David W. Zingg University of Toronto Institute for Aerospace Studies, August 26, 1999.

[14] GAMBIT tutorial guide for GAMBIT 2.2 software package by fluent inc. September 2004

[15] FLUENT Tutorial Guide for fluent software package of FLUENT 6.3.26, by fluent inc. December 2001

Appendix 1 : Software package procedures and used parameter values

Importing model and setting boundary condition in GAMBIT [14]

Select solver type

Solver ➡ fluent 5/6

Import IGES file of the 2d model

FILE ➡IMPORT ➡D:/PROJECT/CROSS FLOW/ DIAM--/MODEL FILE NAME

Eliminate very short edges

GEOMETRY ➡ EDGE ➡ CONNECT/DISCONNECT EDGES

a) Select "All" from the option menu to the right of **Edges**.

b) Select the Real and Virtual (Tolerance) option.

c) Press the Highlight shortest edge button.

GAMBIT will highlight (in white) the shortest edge along with its label in the graphics window.

d) Zoom in near the highlighted edge by pressing the *Ctrl* key while using the mouse to drag a box around the edge.

Remove the shortest edge.

GEOMETRY ➡ VERTEX ➡ CONNECT/DISCONNECT VERTICES

This command sequence opens the Connect Vertices form.

a) Select the Virtual (Forced) option.

b) Pick the two endpoint vertices on the shortest edge.

c) Click Apply.

When GAMBIT *attempts to connect these two vertices, an error message is generated stating that connecting these two vertices can cause invalid geometry. The geometry is protected from such operations by means of a default setting.*

d) Open the **Edit Defaults** form (select **Defaults** from the **Edit** menu on the main menu bar), and change the value of the GEOMETRY VERTEX CONNECT /REMOVE SHORT EDGE variable to 1.
e) Repeat step (c).
This time, GAMBIT *connects the vertices.*
f) Click the **FIT TO WINDOW** command button at the top left of the **Global Control** toolpad to see the full cross flow turbine model in the graphics window.

Make a faces from the lines of the 2d model

OPERATION ➡ GEOMETRY➡ FACE ➡ CREATE FACE FROM WIRE FRAME

Subtracting faces to specify the fluid face

GEOMETRY ➡ FACE ➡SUBTRACT REAL FACES

Creating groups of edges

GEOMETRY ➡ GROUPS ➡ CREATE GROUP
Creating groups of edges

Creating meshes on fluid face

MESH ➡ FACE ➡MESH FACES

Set Boundary Types

Hiding the mesh from the display before setting the boundary types makes it easier to see the edges and faces of the geometry. The mesh is not deleted, but rather removed from the graphics window.
a) Click the **SPECIFY DISPLAY ATTRIBUTES** command button at the bottom of the **Global Control** tool pad.
b) Select the Off radio button to the right of **Mesh** near the bottom of the form.
c) Click **Apply** and close the form.

Set boundary types for the entire cross flow turbine.

ZONES ➡ SPECIFY BOUNDARY TYPES

Set continuum zone types:

ZONES ➡ SPECIFY CONTINUUM TYPES

This opens the specify continuum window:

Exporting the Mesh and Saving the Session

1. Export a mesh file for the turbine.
FILE ➡ EXPORT ➡ MESH

This command sequence opens the Export Mesh File for providing that the File Type is Structured FLUENT 5/6 Grid.

a) Enter the **File Name** for the file to be exported.
b) Click **Accept.**
The file will be written to the working directory.

2. Saving the GAMBIT session and exiting GAMBIT.
FILE ➡ EXIT

Click **Yes** to save the current session and exit GAMBIT.

In summary, the IGES files from Solid Works source were imported to GAMBIT and manipulated using the necessary steps for mesh generation in the fluid face, including boundary types set up, and specification of the **Fluent 5/6** solver. A final mesh file ready for CFD processing was the outcome.

Fluent 6.3

Importing the mesh file from the GAMBIT result and undergoing under-going the analysis [15]

1. Make sure that the user-defined function (UDF) syntax file to define the rigid-body motion of the rotor (blade and pipe) is included in the same working directory. This function was already named as "rotor.c" (Appendix 2). This file will be needed to compile it within FLUENT.
2. Start the 2ddp version of FLUENT either using visual studio command prompt from the working directory or simply going through the start menu.

Step 1: Grid

Read the grid file "file name .msh".

FILE ➡READ ➡CASE
Browsing the right location of ".msh" file in the working directory.

GRID ➡CHECK

Scale the grid.

GRID ➡ SCALE

(a) "in" was selected under Units Conversion from the drop-down list for Grid Was Created In m(meter).
(b) Click Scale to scale the grid.
(c) Click Change Length Units as the working units for length now becomes meters, and then click close.
It must be noted that the numbers shown in the Domain Extents reflect the size of magnified model drawn in Solid Works. Therefore, the numbers should be further scaled down by the geometric scale factor of 1.

Display the grid

DISPLAY ➡ GRID

Click display

Step 2: Units

1. For convenience, define new units for pressure and mass flow.
Pressure, length, and temperature are specified in Pascal, meter, and kelvin respectively. The units for length were already changed while scaling the grid.

DEFINE ➡ UNITS
Set Units

(a) Select ‘pressure’ under Quantities, and ‘psi’ under Units.
(b) Select ‘temperature’ under Quantities, and click ‘f’ under Units.
The Define Unit panel will be displayed.

Step 3: Models

1. Enable a 2D time-dependent calculation.

DEFINE ➡ MODELS ➡ SOLVER

(a) Under Space, click on 2D.
(b) Click on Unsteady under Time.
(c) Keep the default Unsteady Formulation option of 1st-Order Implicit.
Keep in mind that dynamic mesh simulations work only with first order time variant for tri/tetra mesh, re-meshing, and smoothing.
(d) Click on OK.

2. Turn on the Energy Equation for viscous heating properties.
DEFINE ➡ MODELS ➡ ENERGY

3. Turn on the standard k- f turbulence model.
DEFINE ➡ MODELS ➡ VISCOUS

(a) Check on **k-epsilon** as the Model, and use the default setting of Standard under k-epsilon Model.
(b) Check on Viscous Heating under Options.
(c) Click on OK

Step 4: Materials

New material called mild steel is created for housing material. Water and steel were loaded from the FLUENT database for the fluid and solid material properties used to represent the fluid face and the gears.
DEFINE ➡ MATERIALS

(a) In the **Material Type** field, select **solid** from the drop down list.
(b) In the **Name** field, enter **mild steel** and type **m.st** in **Chemical Formula** field.
(c) Specify 7160.9 for the **Density.**
(d) Specify 545.77 for Cpo
(e) Thermal conductivity 42 w/m.k
(f) Click **Change/Create.**
(g) Click **No** for not to overwrite steel on aluminum.

Two other materials **"water-liquid"** as fluid and **"steel"** as solid were uploaded from the FLUENT Database by copying.

Step 5: Operating Conditions

Set the operating pressure to 0 psi
DEFINE ➡ OPERATING CONDITIONS

Step 6: Boundary Conditions

Dynamic mesh motion and all related parameters are specified using the items in the **Define/Dynamic Mesh** submenu, not through the **Boundary Conditions** panel. Here, Pressure inlet at "in" zone and pressure outlet at "out" zone were set up as well as "steel" was chosen as the material for the valve, blade and pipe and housing. "mild steel" was picked up as the material for the housing and "liquid water" for the fluid meshed face. Inlet zone temperature was assumed as 20°C (68f)) and back flow total temperature from the outlet zone was assumed as 25° C (77f). Turbulence intensity (%) and turbulent viscosity ratio for inlet zone were assumed 2% and 2 respectively. For the outlet zone, backflow turbulence intensity (%) and backflow turbulent viscosity ratio were taken as 10 % and 10 respectively. Mass flow rate of 80l/s (80Kg/s), the pressure inlet and pressure outlet were used are gauge pressure of 100000, supersonic pressure of 981000 (145 & 142.3 psi) and 101300 (14.7 psi) Pascal respectively.

DEFINE ➡ BOUNDARY CONDITIONS

1. Set the conditions for the pressure inlet **(inlet). (**145psi gauge total pressure and 142.3 psi as supersonic pressure), Click **OK**
2. Set the conditions for the exit boundary **(outlet).** (14.7 psi as gauge pressure) And check target mass flow rate and put 80 Kg/s in the open space, Click **OK**
3. Set the fluid material **"water liquid"** for the grid face fluid, Get water liquid selecting from the drop down list in Material Name. Click OK.
4. Choose steel as the material for blade and pipe "**blade_and_pipe**" and similarly for valve "**guide valve**". Choose mild steel as the material for housing "**casing**" in the similar way. Click OK for every three wall windows.

Step 7: Mesh Motion

1. Read in and compile the user-defined function (UDF).

DEFINE ➡ USER-DEFINED ➡ FUNCTIONS ➡ COMPILED

(a) Click Add under Source Files,
A Select File panel will show up.
(b) Choose the source code "rotor.c" (Appendix 2) in the Select File panel, and click on OK.
(c) Click on Build in the Compiled UDFs panel,

The user-defined function was already been defined. Compiling the UDF in FLUENT creates a library with the default name "libudf' in the working directory.

(d) Click on **OK** in the dialog box which will show up as shown below. It is just a warning to remove any other "libudf' directory existing in the working directory.

2. Activate dynamic mesh motion and specify the associated parameters.

DEFINE ➡DYNAMIC MESH ➡PARAMETERS ➡DYNAMIC MESH

(a) Select **Dynamic Mesh** under **Model.**
(b) Under **Mesh Methods,** select **Smoothing and Re-meshing.**
FLUENT automatically re-meshes and smoothes the existing mesh zones for use of the different dynamic mesh methods where applicable.
(c) Setting up the parameters under **Smoothing** as follows:
i. Specifying 0.01 for the **Spring Constant Factor.**
ii. Specifying 0.3 for the **Boundary Node Relaxation.**
iii. Keeping up the default specification of 0.0001 for the **Convergence Tolerance.**
iv. Specifying 160 for the **Number** of Iterations.
(d) Setting up the parameters under **Re-meshing** as follows:
i. Under **Options,** be sure that the **Must Improve Skewness** option is selected.
ii. Specify 1.le-15 m3 for the **Minimum Cell Volume.**
iii. Specify 1.2e-08 m3 for the **Maximum Cell Volume.**
iv. Keeping up the default value of 0.6 for the **Maximum Cell Skewness.**
v. Specify 1 for the **Size Re-mesh Interval.**

Any cells exceeding these limits will be re-meshed and smoothed automatically.

(e) Click on **OK.**

(f) Activate spring smoothening factor for quad type element using text command

Define/models/dynamic-mesh-controls/smoothing-parameter/spring-on-all-shapes? yes

3. Specify the motion of the blade and pipe, valve and the housing.
   The motion of blade and pipe and the stationary wall "housing" were specified by using UDFs.
   DEFINE ➡ DYNAMIC MESH ➡ ZONES

(a) Specify the motion of the stationary housing named as 'casing'.

i. Selecting housing 'casing' in the Zone Names drop-down list.
ii. Selecting Stationary under Type.
iii. Click the Meshing Options tab.
vi. Specify 0.005 in for Cell Height.
vii. Click on Create.

(b) Specify the rigid body motion of the blade and pipe

i. Select the blade and pipe named as "blade_and_pipe" in the Zone Names drop-down list,
ii. Under Type, keep the default selection of Rigid Body.
iii. Under Motion Attributes, select rotor in the Motion UDF/Profile drop-down list.
iv. Keep the default values of (0, 0) m for C.G. Location, and 0 for C.G. Orientation. The position of the CG will be updated automatically by FLUENT based on the input of motion.
v. Click on the Meshing Options tab.
vi. Specifying 0.005 in for Cell Height.
vii. Click **Create.**

(c) Specify the motion of the stationary part named as 'valve guide'.

i. Selecting 'valve' in the Zone Names drop-down list.
ii. Selecting Stationary under Type.
iii. Click the Meshing Options tab.
vi. Specify 0.005 in for Cell Height.
vii. Click on Create.

(d) Preview of Mesh Motion

SOLVE ➡ MESH MOTION

(i) Type 0.0001 in Time Step Size and 5 in the Number of Time Steps.
(ii) Check Display Grid under Display Options to see the mesh motion in grid.
(iii) Click on Preview to view the mesh motion in cross flow model with rotational motions in blade and pipe the graphics window of mesh motion in the grid was displayed with message in the FLUENT window screen. Also the stretching, skewing, and collapsing of cells were seen in grid graphics

Step 8: Solution

1. Set the solution parameters.

SOLVE ➡ CONTROLS ➡ SOLUTION.
(a) Keep all default discretization methods and values for under-relaxation factors.
(b) Click on OK.

2. Request that case and data files are automatically saved every 50 time steps.

FILE ➡ WRITE ➡ AUTOSAVE
(a) Set both Autosave Case File Frequency & Autosave Data File Frequency to 50.
(b) In the Filename field, enter the location for file name to save and file name.
(c) Click OK.

3. Enable the plotting of residuals during the calculation.

SOLVE ➡ MONITORS ➡ RESIDUAL
Check on the plot check box under options

4. Initialize the solution.
Initializing the flow field at this point will display contours and vectors that can be used to define animations.

SOLVE ➡ INITIALIZE ➡ INITIALIZE
(a) In Solution Initialization panel, select "inlet" from the drop down lists of
Compute from menu. Then, FLUENT will automatically set up the following parameters from the inlet "inlet" boundary conditions as shown below:

(i) Gauge Pressure to 142.3psi.
(ii) X Velocity to -6.107281\s
(iii) Y Velocity to 0 m\s
(iv) Turbulence Kinetic Energy to 0.02237933
(v) Turbulence Dissipation Rate to 2242969
(vi) Temperature to 68
(vii) Click Init, Apply and Close.

5. Create animation sequences for the static pressure contour plots and velocity vectors plots in the cross flow. Solution animation features of FLUENT were used to save contour plots of the particular animation sequence in every 5 time steps. After completing the calculation, solution animation playback feature could be used to view the animated sequence plots over time.
Basically, there are five types of animation sequence displays over the time; they are grid, contours, vectors, XY plot etc. For this problem, grid animation, velocity and pressure contours, velocity and pressure direction vectors were picked for animation sequences over 5 time steps.

SOLVE ➡ ANIMATE ➡ DEFINE

(a) Increase the number of Animation Sequences to 5.

(b) Under Name, enter grid for the first animation, and pressure for the second one, velocity for the third, press_dir and vel_dir for the latter two.

(c) Under Every, increase the number to 5 for all five sequences.

(d) In the When drop-down list, select Time Step.

(e) Define the animation sequence for the second animation sequence pressure.

i. Click Define on the line for pressure to set the parameters for the sequence.
The Animation Sequence panel will open as:

ii. Below the Storage Type, keep the default selection of Metafile.

iii. Increase the Window number to 1 and click Set.
Graphics window number 1 will be displayed.

iv. Under the Display Type, select Contours.
The Contours panel will be displayed.

v. Under Options, turn on Filled.

vi. In the Contours Of drop-down lists, select Pressure and Static Pressure.

vii. Click Display

viii. Click OK in the Animation Sequence panel.

The Animation Sequence panel will close, and the checkbox in the Active column next to pressure in the Solution Animation panel will become selected.

ix. Click OK in the Solution Animation panel.

(f) Define the animation sequence for the velocity vectors.

i. Click Define on the line for vel_dir to set the parameters for the sequence.
The Animation Sequence panel will open. It is same as pressure contour panel.

ii. Under Storage Type, keep the default selection of Metafile.

iii. Increase the Window number to 2 and click Set.
Graphics window number 2 will open.

iv. Under Display Type, select Vectors.

v. Type 10 in the Scale panel to see the velocity vectors distinctive.
The Vectors panel will open and it will show Min (m/s) and Max (m/s) values when clicking on Display.

vi. Click on Display in the Vectors panel

Velocity Vectors at t = 0 s will be displayed

vii. Click OK in the Animation Sequence panel.
The Animation Sequence panel will be closed, and the checkbox in the Active column next to vel_dir in the Solution Animation panel will become selected.

vii. Click OK in the Solution Animation panel.

6. Set the time step parameters for the calculation.

SOLVE ➡ ITERATE

(a) Set the Time Step Size to 0.001 s.
(b) Increase the Max Iterations per Time Step to 200.
(c) Click Apply.

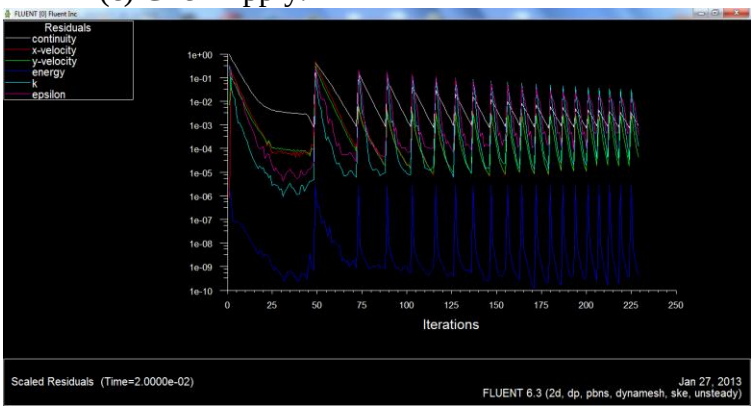

Iteration result graph

7. Save the initial case and data files (file name.cas and cross file name.dat).

FILE ➡ WRITE ➡CASE & DATA

8. Request 20 time steps. For better results at total time t = 1 s, 1000 time steps were set up.

SOLVE ➡ITERATE.

Max Iterations per time step, reporting interval & UDF profile update interval can be changed. The graphics window of iteration will show up which is after time t =0. 02

Step 9: Post-processing

1. Inspect the solution at the final time step.
   (a) Observe the contours of pressure and velocity in the cross flow turbine
   (b) Observe the velocity vectors in the cross flow turbine

2. Optionally, inspect the solution at different intermediate time steps.
   (a) Read in the corresponding case and data files

FILE ➡ READ ➡ CASE & DATA

3. Play back the animation of the pressure contours.

SOLVE ➡ANIMATE ➡ PLAYBACK

(a) In the **Sequences** list, select **pressure.**
The playback control buttons will become active.
(b) Set the slider bar above **Replay Speed** about halfway between **Slow** and **Fast.**
(c) Keep the default settings in the rest of the panel and click the play button (the second from the right in the group of buttons under **Playback).**

Appendix 2: User Defined Function

The user defined function code in c format for dynamic mesh in fluent for the rotation of the rotor at 750 rpm (1.3 rad/s) of the turbine “rotor.c” is shown below

```
/*This code is written in "C"*/
/*UDF starts for the rotor*/
#include "udf.h"
#include "dynamesh_tools.h"
/*UDF starts for Rotational Speed of rotor*/
DEFINE_CG_MOTION(rotor, dt, vel, omega, time, dtime)
{
NV_S (vel,=,0.0);
NV_S (omega,=,0.0);
/*Linear Velocity for blade and pipe*/
vel[0]=0.0;
vel[1]=0.0;
vel[2]=0.0;
/*Angular Velocity for blade and pipe*/
omega[0]=0;
omega[1]=0;
omega[2]=1.3;
/*Messages for Display*/
Message("\nThis is the blade and pipe\n");
Message("\nCG_Omega for rotor: %g, %g, %g\n", omega[0],omega[1],omega[2]);
Message("\nCG Position for rotor: %g, %g, %g\n", NV_LIST(DT_CG(dt)));
Message("\nCG Orientation for rotor: %g, %g, %g\n", NV_LIST(DT_THETA(dt)));
}
/*UDF ends for Rotational Speed of blade and pipe*/
```

ADDIS ABABA UNIVERSITY

SCHOOL OF GRADUATE STUDIES

INSTITUTE OF TECHNOLOGY

DEPARTMENT OF MECHANICAL ENGINEERING

DECLARATION

I, the undersigned, declare that this thesis is my original work and has not been presented for any degree in any university and all the sources of materials used for the thesis have been duly acknowledged.

Endashaw Tesfaye _____ _____

Name Signature Date

January 2013